Article

Current Biology

Lateral Hypothalamic GABAergic Neurons Encode Reward Predictions that Are Relayed to the Ventral Tegmental Area to Regulate Learning

Highlights

- We characterize a GAD-Cre rat, allowing for manipulation of GABAergic neurons
- Optogenetic inhibition of LH GABA prevents learning about reward-predictive cues
- LH GABA inhibition after learning prevents a cue from eliciting motivated behavior
- LH GABA sends cue-elicited expectancy signals to VTA to regulate future learning

Authors

Melissa J. Sharpe, Nathan J. Marchant, Leslie R. Whitaker, ..., Yavin Shaham, Brandon K. Harvey, Geoffrey Schoenbaum

Correspondence

melissa.sharpe@nih.gov (M.J.S.), bharvey@intra.nida.nih.gov (B.K.H.), geoffrey.schoenbaum@nih.gov (G.S.)

In Brief

Sharpe et al. show that LH GABA neurons are critical for acquisition and storage of cue-reward associations. Furthermore, LH GABA neurons relay cue-elicited expectancies to VTA to regulate future learning. This challenges current dogma, which argues that LH produces motivated output as dictated by forebrain regions or hormonal imbalance.

Sharpe et al., 2017, Current Biology *27*, 2089–2100
July 24, 2017 Published by Elsevier Ltd.
http://dx.doi.org/10.1016/j.cub.2017.06.024

Current Biology
Article

Lateral Hypothalamic GABAergic Neurons Encode Reward Predictions that Are Relayed to the Ventral Tegmental Area to Regulate Learning

Melissa J. Sharpe,[1,2,10,*] Nathan J. Marchant,[1,3,10] Leslie R. Whitaker,[1] Christopher T. Richie,[1] Yajun J. Zhang,[1,4] Erin J. Campbell,[5] Pyry P. Koivula,[1] Julie C. Necarsulmer,[1] Carlos Mejias-Aponte,[1] Marisela Morales,[1] James Pickel,[6] Jeffrey C. Smith,[7] Yael Niv,[2] Yavin Shaham,[1] Brandon K. Harvey,[1,10,*] and Geoffrey Schoenbaum[1,8,9,10,11,*]
[1]National Institute on Drug Abuse, IRP, 251 Bayview Boulevard, Baltimore, MD 21228, USA
[2]Princeton Neuroscience Institute, Princeton University, Washington Road, Princeton, NJ 08544, USA
[3]Florey Institute of Neuroscience and Mental Health, University of Melbourne, 30 Royal Parade, Melbourne, VIC 3052, Australia
[4]National Institute on Alcohol Abuse and Alcoholism, IRP, Executive Boulevard No. 402, Rockville, MD 20852, USA
[5]Neurobiology of Addiction Laboratory, School of Biomedical Sciences and Pharmacy, University of Newcastle and the Hunter Medical Research Institute, University Drive, Newcastle, NSW 2308, Australia
[6]National Institute of Mental Health, IRP, 9000 Rockville Pike, Bethesda, MD 20892, USA
[7]National Institute of Neurological Disorders and Stroke, IRP, 9000 Rockville Pike, Bethesda, MD 20892, USA
[8]Department of Anatomy and Neurobiology, University of Maryland School of Medicine, 20 Penn Street, Baltimore, MD 21201, USA
[9]Solomon H. Snyder Department of Neuroscience, John Hopkins University, 401 N. Broadway, Baltimore, MD 21287, USA
[10]These authors contributed equally
[11]Lead Contact
*Correspondence: melissa.sharpe@nih.gov (M.J.S.), bharvey@intra.nida.nih.gov (B.K.H.), geoffrey.schoenbaum@nih.gov (G.S.)
http://dx.doi.org/10.1016/j.cub.2017.06.024

SUMMARY

Eating is a learned process. Our desires for specific foods arise through experience. Both electrical stimulation and optogenetic studies have shown that increased activity in the lateral hypothalamus (LH) promotes feeding. Current dogma is that these effects reflect a role for LH neurons in the control of the core motivation to feed, and their activity comes under control of forebrain regions to elicit learned food-motivated behaviors. However, these effects could also reflect the storage of associative information about the cues leading to food in LH itself. Here, we present data from several studies that are consistent with a role for LH in learning. In the first experiment, we use a novel GAD-Cre rat to show that optogenetic inhibition of LH γ-aminobutyric acid (GABA) neurons restricted to cue presentation disrupts the rats' ability to learn that a cue predicts food without affecting subsequent food consumption. In the second experiment, we show that this manipulation also disrupts the ability of a cue to promote food seeking after learning. Finally, we show that inhibition of the terminals of the LH GABA neurons in ventral-tegmental area (VTA) facilitates learning about reward-paired cues. These results suggest that the LH GABA neurons are critical for storing and later disseminating information about reward-predictive cues.

INTRODUCTION

The motivation to approach particular foods is a learned process [1–7]. Indeed, the learned aspects of eating support a billion-dollar advertising industry. The golden arches of McDonald's send children into a frenzy on the way back from football games, and the distinctive red and white cans of Coca-Cola can be seen in hands around the world. Even in the absence of advertising slogans, the smell of coffee will not instill a craving for caffeine until it has saved you from a morning of unproductivity. In fact, the most basic information about the reinforcing aspects of food is learned [1–5]: newborn rats do not seek water when they are dehydrated; they have to experience water when thirsty to learn that it quenches their thirst [1–5]. The sight and smell of particular foods and drinks only acquire their ability to motivate behavior via a learned process where their intake relieves the physiological need for sustenance [6, 7].

With the psychological nature of eating in mind, it is surprising that research investigating the neural substrates involved in feeding undervalue the potential importance of learning mechanisms and instead tend to describe these systems primarily in reference to the innate motivational drive to feed [8–15]. For example, findings that electrical stimulation of lateral hypothalamus (LH) increases feeding are often used as evidence that this region is a switch for producing the core motivational drive to approach and consume food [8, 10, 11, 16, 17]. Indeed, a role for LH as an output nucleus devoid of learning is pervasive in many studies that have identified a role for LH in appetitive behaviors [9, 18–22].

Yet these effects could easily reflect a more complex learning process in LH itself. Though it is often not noted, in early stimulation studies, rats and mice only show an effect of LH stimulation on food consumption if they have previously experienced

eating in the experimental setting [17, 23, 24]. This is consistent with the notion that stimulation does not just promote indiscriminate feeding but rather impacts on learning to approach particular foods. Further, given the choice, rodents will opt to consume the food previously paired with stimulation rather than another familiar food [17, 23, 25, 26], showing lasting effects of stimulation on food preference. These results suggest that LH stimulation does not automatically produce feeding behaviors. Instead, LH may be involved in the process whereby the rewarding aspects of eating become associated with the specific sensory properties of those foods so that these sensory properties are subsequently able to control motivated behavior to approach and consume the food.

Although some have suggested a role for LH in the psychological aspects of feeding [25, 27–32], this idea has not received widespread acceptance in the field at large. Perhaps part of the reason is that it has been difficult to dissociate a role for this nucleus in learning about food-associated cues from the more traditional role in the production of motivated behavior to approach and consume the food. This is because techniques used to perturb neural activity have traditionally lacked the temporal resolution to distinguish between these accounts; neural activity could only be manipulated across both presentation of food-associated cues and consumption of the food itself. However, optogenetics provides a tool to overcome this hurdle. Recent studies using these techniques have focused on the neuronal specificity of the original LH stimulation effects. Such research has been very valuable in showing us that γ-aminobutyric acid (GABA) neurons are the neuronal population underlying LH-dependent feeding [8, 25]. GABAergic neurons send and receive dense projections from the ventral-tegmental area (VTA) [25, 32]; thus, they are well positioned to play a role in learning. But any such role remains largely speculative.

Here, we took advantage of a newly developed GAD-Cre rat, described in this report, to test this question. In three experiments, we optogenetically inhibited LH GABAergic neurons during a cue-food learning task. In each case, the neurons were inhibited only during cue presentation and not during the subsequent food-delivery period. In one experiment, we inhibited the cell bodies in LH during learning and tested effects in a final probe test without any inhibition. We found reduced responding to the cue with no effects on subsequent responding to or consumption of the food. These results suggest a role for the LH GABA neurons in learning to associate specific sensory information with the rewarding effects of food consumption. In the second experiment, we inhibited the cell bodies in LH only in the final probe test after normal learning. We again found a selective reduction in responding to the cue, showing a role for LH GABA neurons in the expression of the learned information, consistent with an involvement in its storage. Finally, in a third experiment, we inhibited the terminals of the LH GABA neurons in VTA during learning. We found increased responding to the cue, an effect we interpret as showing that reward predictions signaled by LH GABA neurons are contributing the changes in error signaling by VTA dopamine neurons during learning. According to this hypothesis, preventing this signal from reaching VTA produces excessive error signaling, driving the greater learning about the antecedent reward-predictive cue. Together, these studies provide convincing evidence demonstrating that LH GABA neurons are critical for storing and later disseminating information about reward-predictive cues.

RESULTS

The GAD-Cre Rat

To enable the selective labeling and manipulation of GABAergic neurons in the rat brain, we developed a transgenic rat on a Long-Evans background. This rat expresses Cre recombinase from the glutamate decarboxylase 1 (GAD1) promoter—one of two genes encoding the GAD enzyme that converts glutamate to GABA. A bacterial artificial chromosome (BAC) containing the rat GAD1 gene was recombined to express Cre-recombinase in place of the GAD67 protein encoded by GAD1 gene (see Figure 1A) and microinjected into rat embryos, resulting in 3/75 founder rats. Only one of the three founder rat lines, LE-Tg(GAD1-iCre)3Ottc (referred to as "GAD-Cre" rat herein) had a single copy of the Cre transgene per rat genome and demonstrated relatively high co-expression of Cre and GAD1 mRNA in the midbrain (76% ± 11%), LH (80% ± 6%), and brainstem (85% ± 6%; see Figure S1 and STAR Methods). The same analysis in the anterior cingulate cortex, however, revealed lower fidelity of co-expression between Cre and GAD1 mRNA (32% ± 8%; data not shown). Injection of AAV-EF1a-DIO-Nuc-eYFP (nYFP), a Cre-dependent AAV expressing nuclear-localized yellow fluorescent protein, into several brain regions resulted in subset of nYFP-expressing cells. Co-labeling of nYFP-injected brain sections for GAD1 mRNA by fluorescence RNA in situ hybridization showed that the majority (87% ± 10%) of nYFP-protein-expressing cells expressed GAD1 mRNA in the LH (see Figures 1B–1E) and midbrain (see Figure S3). We also used this method to clarify whether our infected cells expressing GAD1 expressed other markers of GABA neurons. We found a high degree of co-localization between nYFP-expressing cells and expression of both GAD2 and the vesicular GABA transporter (VGAT) (91% ± 7%; see Figures 1F–1I). In addition, analyses of endogenous co-expression of these markers revealed high co-localization of GAD1 and GAD2 (100% ± 0%), GAD1 and VGAT (100% ± 0%), and GAD2 and VGAT (98% ± 2%; see Figure S2), and there was a very low co-localization with VGAT and the vesicular glutamate transporter (VGLUT2) (1% ± 1%) (see Figure S2), showing that the GABAergic neurons in the LH are a different population of cells than the glutamate-releasing neurons in the LH. These analyses show that there is a high co-expression of both Cre and GAD1 throughout the brain and demonstrate that GAD1 cells have a GABAergic phenotype.

We also wanted to ensure that LH GABAergic neurons do not express MCH or ORX, two peptides that have been extensively studied in LH [8, 27]. Similarly to other recent studies in mice [8], we found little overlap between neurons infected with eYFP and cells releasing MCH or ORX (1.2% and <1% of eYFP+ neurons also stained for MCH [n = 6] and ORX [n = 3], respectively; see Figures 1J and 1K). These data support the proposal that the effects found behaviorally in the following sections were due to a specific manipulation of GABAergic neurons that did not co-release MCH or ORX.

Finally, to confirm that light does inhibit the firing of cells containing AAV- EF1α-DIO-eNpHR3.0-eYFP (NpHR) in these GAD-Cre rats, we also performed ex vivo electrophysiology. Exposure to light inhibited firing in NpHR-eYFP+ LH neurons

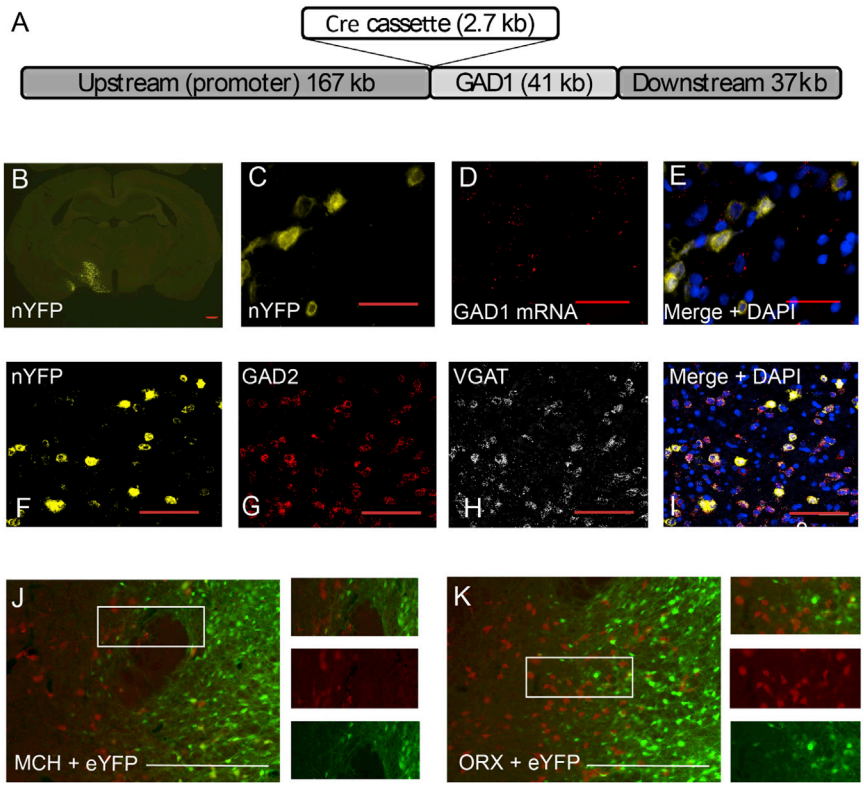

Figure 1. Basic Characterization of the GAD-Cre Rat

(A) BAC DNA construct used to generate GAD1-Cre rats.

(B) Coronal section showing nYFP expression in LH 2 weeks after AAV injection. The scale bar represents 0.5 mm.

(C and D) Colocalization of (C) nYFP protein fluorescence (D) and GAD1 mRNA.

(E) Merged image of nYFP (yellow), GAD1 mRNA (red), and total nuclei (blue; DAPI) shows GAD1 mRNA associates with nYFP signal in the LH.

(F–H) Colocalization of (F) nYFP protein fluorescence, (G) GAD2 mRNA, and (H) VGAT mRNA.

(I) Merged image of nYFP (yellow), GAD2, and VGAT; scale bars (C–I) = 100 μm.

(J) Neuronal overlap between eYFP-infected (green) and MCH-releasing neurons (red), where only 1.2% of eYFP+ neurons also stained for MCH.

(K) Similar analyses assessing the proportion of ORX-releasing cells (red), which also expressed eYFP (green); less than 1% of eYFP+ neurons co-stained ORX. The scale bars represent 20 μm. See also Figures S1 and S2 and Movies S1 and S2.

following depolarizing current injection but had no effect on firing frequency in NpHR-eYFP- LH neurons (mean % inhibition [±SEM]: eYFP− 6.7 [4.1]; eYFP+ 97.92 [2.1]; $t(5) = 21.4$; $p < 0.0001$; see Figure 2B, left). Resting membrane potential was hyperpolarized following light exposure in NpHR-eYFP+, but not NpHR-eYFP− LH neurons (mean mV [±SEM]: eYFP− −0.22 [0.25]; eYFP+ −15.23 [3.2]; $t(8) = 5.9$; $p = 0.003$; see Figure 2B, right). Further, we also wanted to confirm that neurons expressing Cre are capable of releasing GABA. To do this, we recorded post-synaptic $GABA_A$-mediated currents downstream in VTA while stimulating LH GABA neurons infected with AAV-DIO-EF1α-ChR2-eYFP (ChR2). We found that stimulating LH GABA increased inhibitory post-synaptic currents (IPSCs) in VTA, which were blocked by the addition of the GABAergic antagonist picrotoxin (PTX) (mean IPSC amplitude [±SEM]: baseline 182.26 [39.62]; +PTX 8.15 [1.72]; $t(4) = 4.37$; $p = 0.01$; see Figures 2C and 2D).

GABAergic Projections from LH

A Cre-dependent AAV expressing membrane-localized GFP, AAV-EF1a-DIO-Mem-AcGFP, was injected into the LH of the GAD-Cre rats to label GABAergic neurons, including their projections. We used the TissueCyte system, a whole-brain imaging system that couples a two-photon microscope with serial sectioning by vibratome [33]. Following a unilateral injection into the LH, membrane-GFP was detected ipsilaterally with minimal cortical labeling on the contralateral side. This showed intense membrane-GFP labeling in LH and lateral habenula, amygdala (see Figure 3D), and the bed nucleus of the stria terminalis (see Figure 3C). Membrane-GFP labeling was observed in VTA within the parabrachial pigmented area (see Figure 3E), septal regions (see Figure 3B), and ventral-lateral periaqueductal gray (see Figure 3F), and lateral infralimbic (IL) and prelimbic (PL) cortices (mPFC; see Figure 3A). Collectively, these data demonstrate that unilateral injection of AAV serotype 1, encoding a membrane GFP, into the of LH of GAD-Cre rats results in ipsilateral fluorescent labeling that extends both anterior and posterior while remaining along the medial wall (see also Movies S1 and S2).

Optogenetic Inhibition of LH GABA Neurons Attenuates the Acquisition and Expression of Pavlovian Associations

In the behavioral experiments described below, we first trained all rats to enter the food port, where they received 30 45-mg sucrose pellets across a 1-hr period. As food is delivered, rats can hear the auditory turn of the pellet dispenser, and they learn that this predicts pellet delivery during this food-shaping session. Following food-cup shaping, rats underwent conditioning for 12 sessions. In each session, rats received six trials each of two 10-s auditory cues presented individually (tone or siren; counterbalanced): one was immediately followed by delivery of two sucrose pellets (termed the "CS+"), and one was presented without food (termed the "CS−"). As rats learn that the CS+ reliably predicts food, they spend more time in the food port in anticipation of food during presentation of the CS+. This is the dependent variable. After conditioning, rats received an extinction test. Here, both cues were presented individually without food. This test was designed to examine the rats' ability to predict food delivery without reward feedback. In our first experiment, we optogenetically inhibited LH GABA neuron activity during presentation of both the CS+ and CS− during conditioning. In our second experiment, we inhibited LH GABA activity during the cue test after normal conditioning. In both

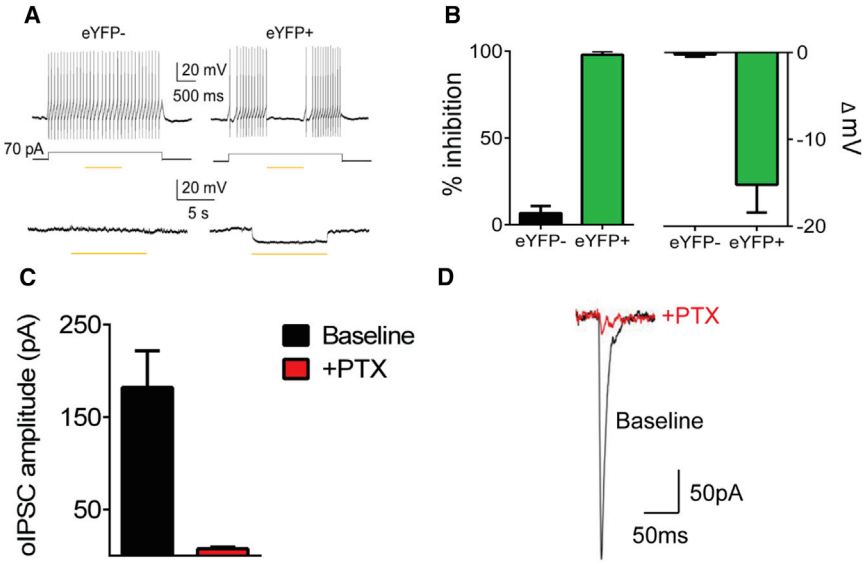

Figure 2. Effects of Light Delivery on Neuronal Activity and GABA Release

(A) Top: there was no effect of light on firing rate following depolarizing current injection in LH neurons not expressing NpHR-eYFP− (eYFP−; n = 3). However, in NpHR-eYFP+ LH neurons (n = 4), introduction of light during depolarizing current injection inhibited firing. Bottom: resting membrane potential in NpHR-eYFP− neurons is unchanged by light exposure (mean ± SEM; −0.22 ± 0.25 mV; n = 6), whereas resting membrane potential is hyperpolarized in NpHR-eYFP+ neurons (mean ± SEM; −15.23 ± 3.2 mV; n = 4).

(B) Left: averaged data from sample in Figure 2A, top right: averaged data from Figure 2A, bottom.

(C) Light stimulation of LH GABA terminals produces an optically evoked IPSC in VTA neurons, which is blocked by addition of $GABA_AR$ antagonist picrotoxin (PTX; mean ± SEM).

(D) Example trace from an optically evoked IPSC in VTA neurons following LH GABA terminal stimulation that is blocked by PTX.

experiments, we used two groups of rats in a factorial experimental design with the between-subjects factors of virus type (NpHR and eYFP) and the within-subjects factor of cue (CS+ and CS−). Thirty-two Long-Evans GAD-Cre rats were trained in these experiments. Prior to training, all rats underwent surgery to inject virus and implant optic fibers targeting the LH. AAV-EF1α-DIO-eNpHR3.0-eYFP [34] (NpHR; n = 16) or AAV-EF1α--DIO-eYFP (eYFP; n = 16) was injected into the LH of GAD-Cre rats (see Figures 4A and 4B). After surgery and recovery, rats were food restricted until their body weight reached 85% of baseline, and then they began conditioning.

Effect of Optogenetic Inhibition of LH GABA Neurons on Acquisition of Pavlovian Associations

In the first experiment, we delivered the laser continuously into the LH of all rats (532 nm; 16–18 mW output; Shanghai Laser & Optics Century) during presentations of both cues. Rats in the eYFP group learned to approach the food cup during cue presentation. This was evident as an increase in time spent in the food port during presentation of the CS+ relative to the CS− across sessions (see Figure 5A). Rats in the eYFP group also spent more time in the food cup during presentation of the CS− relative to baseline rates (when no stimulus was presented; see Figure 5A). This generalization of learning from the CS+ to the CS− is not unusual for cue-food learning tasks, particularly when using cues in the same modality as we did here [35]. By the final day of conditioning, the eYFP rats were spending a higher proportion of time in the food port during presentation of the CS+ than during presentation of the CS− (see Figure 5A).

In contrast, inhibition of LH GABA neurons during cue presentation impaired learning in rats in the NpHR group. This was evident as a significant reduction in time spent in the food port during presentation of the CS+ throughout conditioning (see Figure 5B). Interestingly, the NpHR rats showed some generalization of learning to the CS−, and responding to the CS− was also reduced in NpHR rats relative to the eYFP group (see Figure 5B). This suggests that the generalization of learning across the two cues was similarly susceptible to LH GABA inhibition. Importantly, an effect of LH GABA inhibition on CS− responding is to be expected if inhibiting these neurons affects learning, because this generalized responding is also learned (as indicated by higher levels of responding during presentation of this cue relative to the pre-CS baseline period). There was no impact of the inhibition on responding in the baseline pre-CS period, as compared with the eYFP group.

Statistical analyses supported these observations. A three-factor ANOVA (cue × session × group) of time spent in the food port across conditioning sessions during the CS+, CS−, and baseline pre-CS period showed a main effect of cue ($F_{(2,28)}$ = 56.3; $p < 0.01$), session ($F_{(11,154)}$ = 2.5; $p < 0.01$), and group ($F_{(1,14)}$ = 5.2; $p < 0.04$). There were also significant interactions between cue and group ($F_{(2,28)}$ = 3.6; $p < 0.05$) and cue and session ($F_{(22,308)}$ = 3.2; $p < 0.01$). Follow-up pairwise comparisons showed the source of the interaction between cue and group was due to a significant between-group difference in responding to the CS+ ($F_{(1,14)}$ = 5.8; $p < 0.05$), a trend toward a reduction in responding to the CS− ($F_{(1,14)}$ = 3.9; $p < 0.07$), and no difference in responding during the baseline pre-CS period ($p > 0.1$). A two-factor ANOVA (cue × group) on responding during the CS+ and CS− on the last day of conditioning showed a main effect of cue ($F_{(1,14)}$ = 8.8; $p < 0.01$) and no significant interaction between cue and group ($p > 0.1$) but rather a main effect of group ($F_{(1,14)}$ = 5.9; $p < 0.05$).

Critically, in marked contrast to the deficit in time spent in the food port during presentation of the CS+ or the CS− in the NpHR group relative to the eYFP group, rats in both groups spent an equally high proportion of time in the food port during food delivery *after* presentation of the CS+ (see Figures 5C and 5D). That is, after termination of the CS+, rats in the NpHR group heard the audible turn of the pellet dispenser during food delivery and were motivated to enter the food port and consume the food. Thus, the deficit in responding during the CS+ and CS− in the NpHR group occurred despite normal food consumption immediately after termination of both the CS+ and the laser. A two-factor ANOVA (cue × group) on time spent in the food port during food delivery on the last day of conditioning showed a main effect of cue ($F_{(1,14)}$ = 11.7; $p = 0.004$) but no

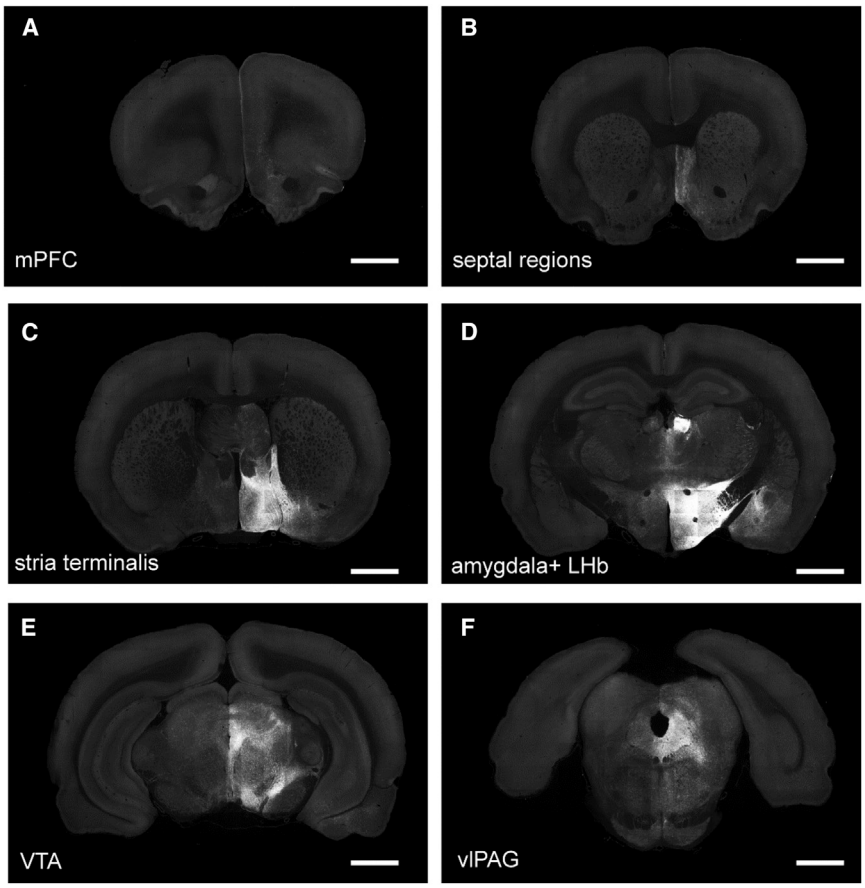

Figure 3. Projections from Virally Transduced GABAergic Neurons in LH

AAV1-EF1a-DIO-mem-AcGFP was injected into the LH, and brain tissue was imaged 2 weeks later using whole-brain TissueCyte system. There was intense membrane-GFP labeling in LH and lateral habenula and amygdala (D) and in the bed nucleus of the stria terminalis (C). Membrane-GFP labeling was also observed in VTA within the parabrachial pigmented area (E), septal regions (B), ventral-lateral periaqueductal gray (F), and lateral infralimbic (IL) and prelimbic (PL) cortices (mPFC; A). Views of stitched fields of coronal sections are shown. The scale bar represents 2 mm. See also Movies S1 and S2 for LH GABA projections throughout the brain, and Figure S3 for VTA GABA projections.

main effect of group ($p > 0.1$) or an interaction between the two factors ($p > 0.1$).

Following conditioning, all rats were given a test in which both cues were presented without food delivery. This test was designed to investigate whether the earlier deficit in responding in the NpHR group in fact reflected a failure to learn or was simply due to a temporary decline in motivation or inhibition of locomotor behavior produced by LH GABA inhibition during the conditioning sessions. Thus, no laser was delivered during this test, ensuring that LH GABA neurons could function normally in all rats. Consistent with an impairment in learning, the NpHR group continued to spend significantly less time in the food cup during presentations of both the CS+ and CS− than did rats in the eYFP group (Figures 5E and 5F). Accordingly, a two-factor ANOVA (cue × group) showed a main effect of cue ($F_{(1,14)} = 15.7$; $p < 0.01$), a main effect of group ($F_{(1.14)} = 15.7$; $p < 0.01$), and no interaction ($p > 1$).

Effect of Optogenetic Inhibition of LH GABA Neurons on Expression of Pavlovian Associations

Our first experiment demonstrated that LH GABA neurons are necessary for hungry rats to learn to associate sensory information with the rewarding aspects of food. Specifically, we found that optogenetic inhibition of LH GABA neurons during conditioning disrupted the ability of rats to learn to expect delivery of food following presentation of a cue that predicted food delivery. These results suggest a reinterpretation of the more conventional role of LH in promoting motivated output as reflecting learning. However, they do not distinguish between a restricted role in learning and a broader role in the storage of the associative information in the LH GABA population itself. To examine this question, we allowed rats to acquire a cue-food association normally, using the same behavioral training procedure as our first experiment and then we inhibited LH GABA neurons during cue presentation in the extinction test after conditioning. If LH GABA neurons are involved in storing these learned associations, then inhibiting these cells during cue presentation should also disrupt cue-elicited food-port entry.

During conditioning, all rats acquired the conditioned response of entering the food port during cue presentation. This was indexed by greater time spent in the food port during CS+ presentation relative to CS− presentation as conditioning progressed. There were no group differences in rates of learning or time spent in the food port during presentations of the cues across learning (see Figures 6A and 6B). The rats again spent more time in the food port during presentation of the CS− relative to the baseline pre-CS period (see Figures 6A and 6B), suggesting that, as in experiment 1, there was some generalization of learning across the auditory cues. Nevertheless, by the final session of conditioning, all rats were exhibiting robust levels of responding during presentation of the CS+ relative to the CS− (see Figures 6A and 6B). A three-factor ANOVA (cue × session × group) on time spent in the food port across conditioning sessions during the CS+, CS−, and pre-CS baseline period showed a main effect of cue ($F_{(2,28)} = 57.6$; $p < 0.01$) and session ($F_{(11,154)} = 3.8$; $p < 0.01$) but no main effect of group ($p > 0.1$). There was a significant interaction between cue and session ($F_{(22,308)} = 3.8$; $p < 0.01$) but no other significant interactions ($p > 0.1$). A two-factor ANOVA (cue × group) on responding during the CS+ and CS− on the last day of conditioning showed a main effect of cue ($F_{(1,14)} = 30.0$; $p < 0.01$) but no interaction with group or any main effect of group ($p > 0.1$). Additionally, on the final day of conditioning, all rats spent a high proportion of time in the food cup during food delivery after presentation of the CS+, and there were no differences between groups

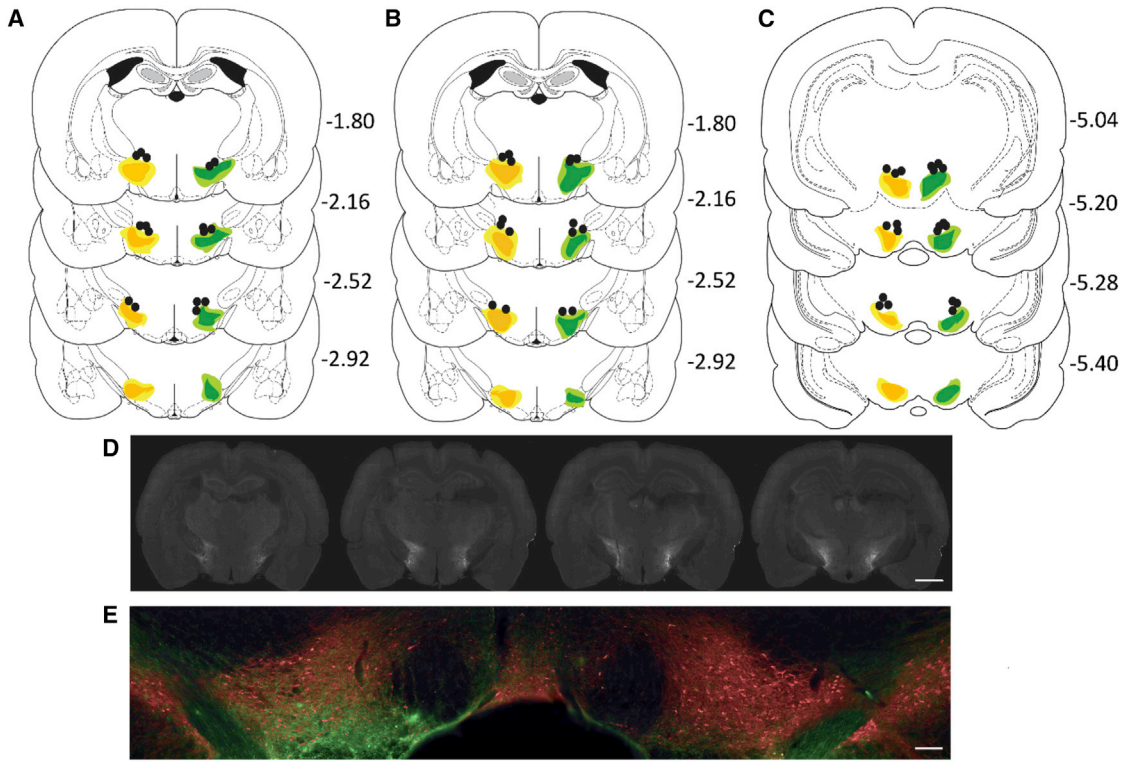

Figure 4. Immunohistochemical Verification of Cre-Dependent NpHR and eYFP and Fiber Placements for Behavioral Experiments 1–3

Top images: unilateral representation of the bilateral fiber placements and virus expression in each group (mm). Fiber implants (black circles) were localized in the vicinity of eYFP (green) and NpHR (orange) expression in VTA. The light shading represents the maximal and the dark shading indicates the minimal spread of expression at each level.

(A) Schematic of neuronal virus expression and fiber placement in the LH subjects from experiment 1.

(B) Schematic of neuronal virus expression and fiber placements in the LH of subjects from experiment 2.

(C) Schematic of terminal virus expression and fiber placement in the VTA of subjects used in experiment 3.

(D) Middle image: visualization of NpHR expression in LH in one subject; scale bar 2 mm.

(E) Bottom image: injection of NpHR into LH GABA neurons produces extensive labeling of terminals (eYFP; green) in VTA adjacent to dopamine neurons (tyrosine hydroxylase+; red); scale bar 400 μm.

(see Figures 6C and 6D). A two-factor ANOVA (cue × group) showed a main effect of cue ($F_{(1,14)}$ = 81.9; $p < 0.01$) but no main effect or any interaction with group ($p > 0.1$).

Following conditioning, all rats were given a test in which both cues were presented without food delivery. In this test session, we delivered the laser continuously into the LH of all rats (532 nm; 16–18 mW output) during presentation of both cues. We found that our NpHR group spent significantly less time in the food port during presentation of both the CS+ and CS− than did rats in the eYFP group (Figures 6E and 6F). Accordingly, a two-factor ANOVA (cue × group) showed a main effect of cue ($F_{(1,14)}$ = 15.9; $p < 0.01$) and a main effect of group ($F_{(1,14)}$ = 5.2; $p < 0.05$) but no interaction between these factors ($p > 0.1$). Combined, these experiments show that LH GABA neurons are critically involved in both the acquisition and expression of cue-reward associations.

Optogenetic Inhibition of LH GABA Neurons Does Not Affect Locomotor Activity

We found that the deficit in responding during conditioning in experiment 1 was maintained in an extinction test without laser-mediated inhibition of LH GABA neurons. This suggests that the reduction in responding during conditioning was indeed the result of a deficit in acquiring associative information rather than a deficit in locomotor activity. To confirm that there was no effect of LH GABA inhibition on locomotor activity, we implanted fiber optics into the LH of rats with bilateral expression of NpHR also in LH. These rats were placed in the chambers used for the appetitive procedures described above, equipped with four infrared photobeams to register movement in the box, and we activated the laser for 10-s periods. A comparison of locomotion activity during the laser period with that during the 10-s periods immediately before and after the laser was delivered found no change in locomotion (ANOVA across the three time periods, $F < 1$; see Figure S4).

Inhibition of the Terminals from LH GABA Neurons in VTA during Learning Facilitates the Development of Cue-Food Associations

Experiments 1 and 2 indicate that LH GABA neurons are involved in the acquisition and storage of learned cue-food associations. One major projection of these neurons, evident in our characterization of their targets (see Figure 3), is the VTA. VTA dopamine neurons are proposed to signal reward predictions to mediate learning

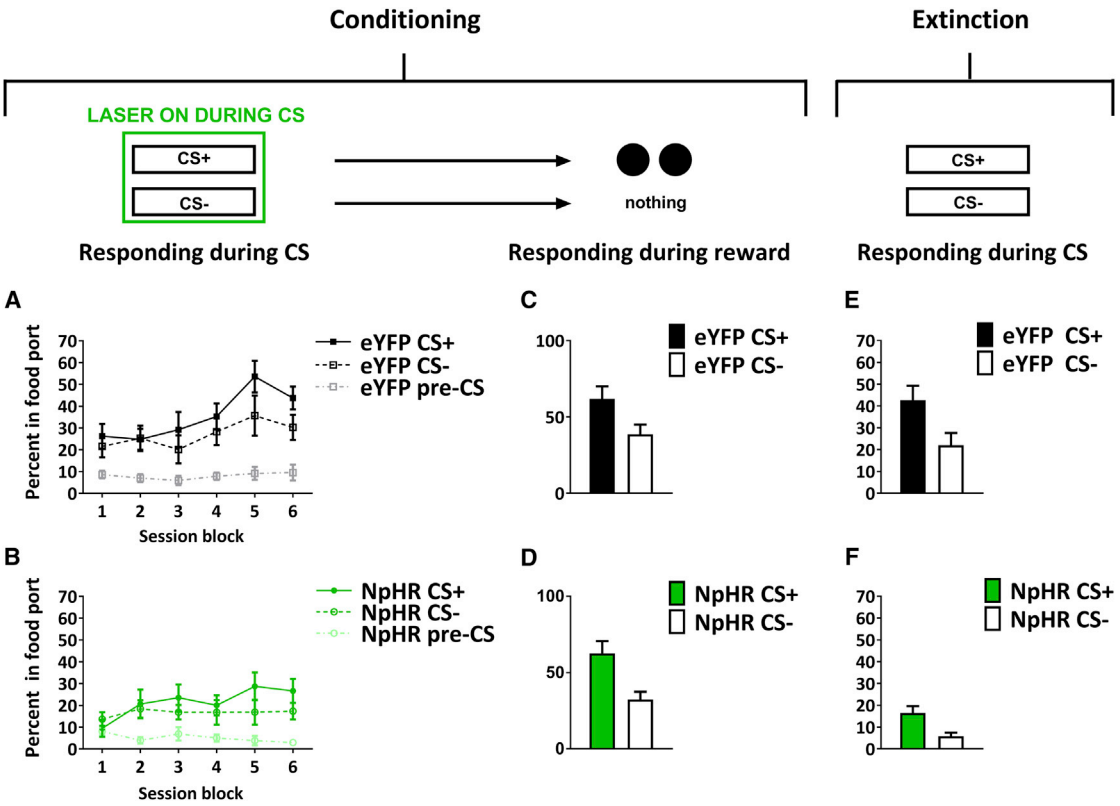

Figure 5. Inhibition of LH GABA Neurons Disrupts Learning of Cue-Food Associations

The figures show percent time spent in the food port (mean ± SEM) during cue presentation (A and B) or reward delivery (C and D) during conditioning or cue presentation during the extinction test (E and F). Despite normal levels of responding during reward delivery demonstrating that all rats experienced the cue and reward in close temporal succession, inhibition of LH GABA neurons (NpHR group) attenuated learning. This effect was maintained in an extinction test without laser-mediated inhibition of LH GABA neurons. See also Figure S4.

about reward-paired cues [36]. These neurons fire in proportion to the discrepancy between the actual and predicted reward. Blocking input about predicted reward during learning should result in larger error signals. We reasoned that if LH GABA neurons signal these reward predictions, then preventing this information from being received in VTA might result in increased rather than decreased learning. That is, if we could selectively deprive the VTA of these predictions (while leaving LH GABA cell bodies and any other regions involved in this process online and free to store learned associations between the cue and reward), then this might result in greater learning about the antecedent cue. To investigate this hypothesis, we again trained rats in our simple cue-reward procedure, inhibiting the terminals of LH GABA in VTA during the presentation of both cues and not reward delivery.

We used two groups of rats in a factorial experimental design with the between-subjects factors of virus type (NpHR and eYFP) and the within-subjects factor of cue (CS+ and CS−). Twenty Long-Evans GAD-Cre rats were trained in these experiments. Prior to training, all rats underwent surgery to inject virus into LH and implant fiber optics targeting the VTA. AAV-EF1α-DIO-eNpHR3.0-eYFP (NpHR; n = 9) or AAV-EF1α-DIO-eYFP (eYFP; n = 11) was injected into the LH of GAD-Cre rats (see Figure 4C). After surgery and recovery, rats were food restricted until their body weight reached 85% of baseline, and then they began conditioning. An important difference between this experiment and the previous two experiments is that we gave the rats only one conditioning session a day instead of two per day in experiments 1 and 2. The purpose of this manipulation was to slow rates of learning to more clearly observe the proposed facilitation of learning that this manipulation will produce.

Rats in the eYFP group learned to approach the food cup during cue presentation, exhibiting an increase in time spent in the food port during presentation of the CS+ relative to the CS− across sessions (see Figure 7A). Rats in the eYFP group also spent more time in the food cup during presentation of the CS− relative to baseline rates (see Figure 7A). As expected, rates of learning were slower in this experiment relative to experiments 1 and 2 (see Figures 5A and 6A). Regardless, by the final day of conditioning, the eYFP rats were spending a higher proportion of time in the food port during presentation of the CS+ than during presentation of the CS− (see Figure 7A).

Rats in the NpHR group demonstrated a similar pattern of responding, also learning to approach the food cup during the CS+ during conditioning. However, over the sessions the NpHR rats showed higher levels of responding during CS+ presentation than the eYFP control group (see Figure 7B).

These observations were confirmed by statistical analyses. A three-factor ANOVA (cue × group × session) on responding during the CS+ and CS− elicited a main effect of cue ($F_{(1,18)} = 28.8$; $p < 0.001$), a main effect of session ($F_{(6,108)} = 7.5$; $p < 0.001$), a

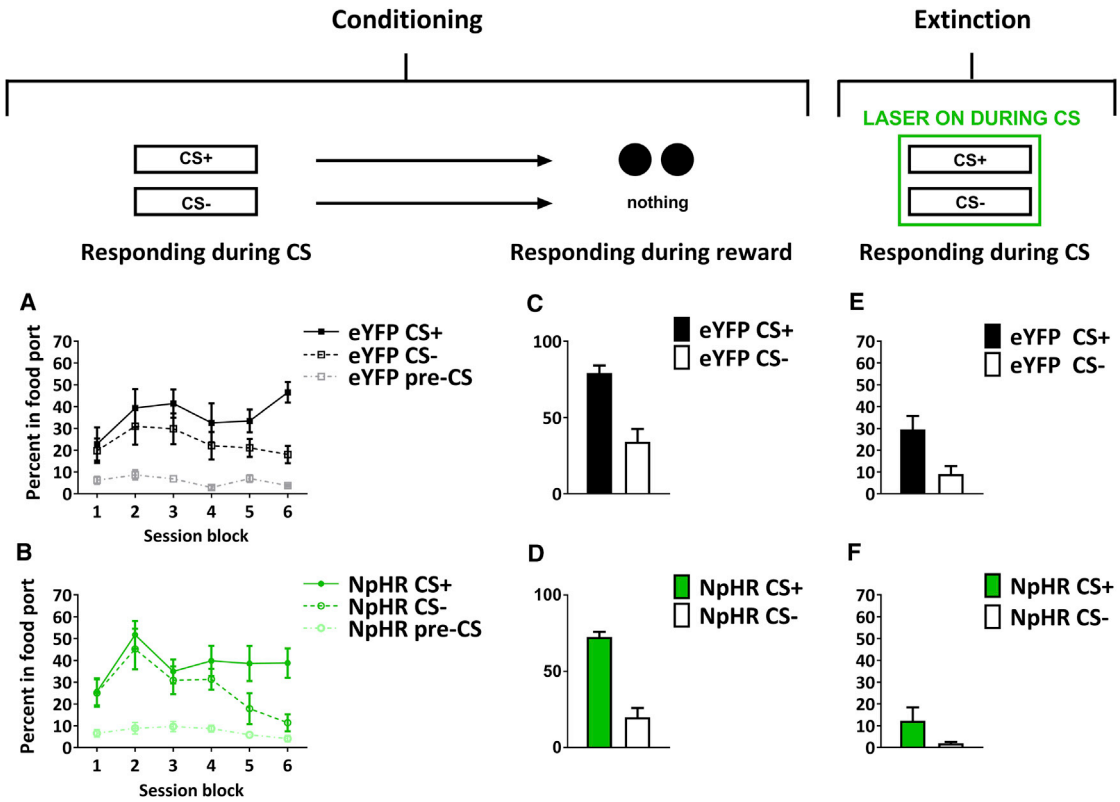

Figure 6. Inhibition of LH GABA Neurons Disrupts the Expression of Learned Cue-Food Associations

The figures show percent time spent in the food port (mean ± SEM) during cue presentation (A and B) or reward delivery (C and D) during conditioning or cue presentation during the extinction test (E and F). All rats acquired the conditioned response in the absence of laser-mediated inhibition of LH GABA neurons. However, when LH GABA was inhibited in the extinction test after normal learning has taken place, rats without LH GABA activity (NpHR group) showed a significant reduction in responding toward the predictive cue. See also Figure S4.

cue × session interaction ($F_{(6,108)}$ = 14.1; p < 0.001), and a three-way cue × group × session interaction ($F_{(6,108)}$ = 3.0; p < 0.02). Further, a cue × group analysis of data from the final session of conditioning elicited a significant main effect of cue ($F_{(1,18)}$ = 36.7; p < 0.001) and a significant cue × group interaction ($F_{(1,18)}$ = 6.8; p < 0.02) but no main effect of group ($F_{(1,18)}$ = 2.8; p = 0.11) Thus, rats in the NpHR group exhibited higher levels of responding to the CS+ in the later stages of conditioning, as if the LH GABA relays an expectation signal to VTA to regulate the dopaminergic teaching signal.

This between-group difference in responding during cue presentation occurred despite normal levels of responding during reward delivery (Figures 7C and 7D). A cue × group ANOVA on responding in the food cup during reward elicited a main effect of cue ($F_{(1,18)}$ = 112.3; p < 0.001) but no cue × group interaction ($F_{(1,18)}$ = 0.8; p = 0.38) or any main effect of group ($F_{(1,18)}$ = 1.3; p = 0.27). Thus, increased conditioned responding to the CS+ was not secondary to elevated responding to the reward.

To confirm that the increased conditioned responding reflected learning, we subsequently continued conditioning the rats for several sessions without laser-mediated inhibition of LH GABA terminals in VTA. During the early sessions, we found that the elevation in responding to cue presentation in NpHR rats was maintained, demonstrating that the greater responding toward the cue in the NpHR group was due to a lasting impact of inhibition of the LH GABA terminals in VTA on learning about cue-reward associations (Figure 7E versus 7F, early). A cue × group × laser ANOVA comparing responding during the final two sessions of conditioning with the laser and the early sessions without the laser elicited a significant main effect of cue ($F_{(1,18)}$ = 33.7; p < 0.001) and a cue × group interaction ($F_{(1,18)}$ = 6.4; p < 0.021) but no group × laser interaction ($F_{(1,18)}$ = 0.4; p = 0.524).

However, with continued training in the absence of inhibition, responding in controls caught up with that in the NpHR rats (Figure 7E versus 7F, late) such that a comparison with the end of the laser training yielded a main effect of cue ($F_{(1,18)}$ = 27.6; p < 0.001), a cue × laser interaction ($F_{(1,18)}$ = 12.6; p < 0.02), and a significant three-way cue × group × laser interaction ($F_{(1,18)}$ = 9.5; p < 0.01). This demonstrated that the change in responding to the CS+ across the conditioning sessions without the laser in the eYFP group was not seen in the NpHR group. In summary, these data are consistent with the hypothesis that LH GABA sends predictions about upcoming food reward to the VTA, and this signal regulates learning about reward-paired cues.

DISCUSSION

Validation of the GAD-Cre Rat

Here, we have described the creation of a novel transgenic rat that expresses Cre-recombinase under the control of

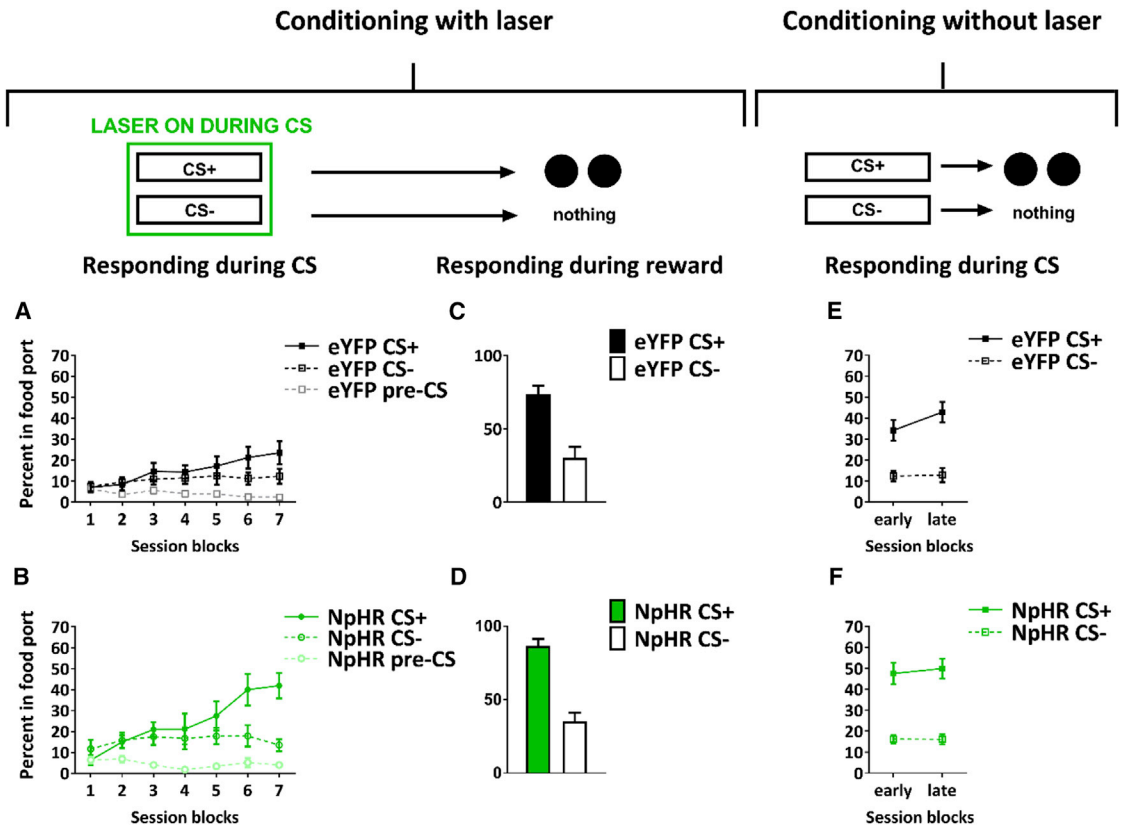

Figure 7. Inhibition of Terminals from LH GABA Neurons in the VTA

The figures show percent time spent in the food port (mean ± SEM) during cue presentation (A and B) or reward delivery (C and D) during conditioning with laser-mediated inhibition of LH GABA terminals in VTA or during cue presentation in conditioning without laser-mediated inhibition of LH GABA terminal in VTA (E and F). Rats in the NpHR group demonstrated significantly greater learning when LH GABA terminals in VTA were inhibited during conditioning. However, when this inhibition was released, these rats ceased learning.

the GAD-1 promoter. Our characterization of the rat primarily focused on the GABAergic neurons of the LH; however, we also surveyed other brain regions for the expression of Cre recombinase by fluorescent in situ hybridization and functional recombination of AAV vectors containing Cre-dependent fluorescent proteins. Overall, we saw a high degree of overlap between Cre expression and GAD1 mRNA in the LH, midbrain, and brainstem. Further, we found a high degree of co-localization between GAD1, GAD2, and VGAT mRNA in LH, demonstrating that GAD1 cells in LH have a GABAergic phenotype. Additionally, we have also characterized the GABAergic projections from LH to the rest of the brain. These LH GABA projections include the VTA, LHb, bed nucleus of the stria terminalis, and septal regions. Thus, the GAD-Cre rats represent a powerful tool for studying GABAergic neurons and their projections in the rat, although future studies should validate Cre expression in the brain region of interest.

Inhibition of LH GABA Neurons during Cue Presentation and Not Reward Disrupts the Encoding and Retrieval of Learned Cue-Reward Associations

Using these rats, we found that optogenetic inactivation of LH GABAergic neurons during presentation of a neutral cue disrupted the ability of rats to learn to use the cue to predict food delivery. This reduction occurred despite normal behavior (food cup entry and food consumption) when the food was delivered immediately after cue presentation, suggesting that all rats experienced the rewarding aspects of food presentation similarly. Nevertheless, inactivation of LH GABA neurons prevented the cue from acquiring the ability to motivate the learned response to approach the reward location. This deficit persisted in a test session, in which the LH GABA neurons were not inhibited, demonstrating that the impairment was not due to a transient effect of inhibition on motivation, sensory perception, attention, or locomotor activity, instead suggesting that inactivation impaired the ability of animals to acquire the underlying cue-reward association. Further, inhibition of LH GABA neurons only during the test session after normal learning also reduced the ability of the reward-paired cue to motivate food seeking. Thus, the effect of inhibiting LH GABA neurons during learning was not secondary to loss of learning downstream. Overall, these data indicate that LH GABA neurons are part of a circuit that stores the association between the sensory stimulus and food reward.

The motivation to approach a particular food is the result of a learning process whereby the sensory properties of the food—its sight, smell, and texture, for example—become associated with the rewarding aspects of its consumption [1–3, 6, 7]. For

example, newborn rats do not seek water when they are dehydrated, they have to experience water when thirsty to learn that it quenches their thirst [1, 3]. Viewed in this light, a parsimonious account of current and prior results would involve LH GABA neurons in the process whereby specific sensory information, whether direct attributes of food reward or artificial cues paired with the foods, become predictive of the rewarding aspects of food consumption. Here, we specifically used a Pavlovian conditioning procedure so that we could temporally separate the cue and food and dissociate a role for LH in the motivation to feed and learning about food associates. However, we would expect that inhibition of activity of LH GABA neurons would generally reduce learning about all predictors of food, even when these predictors are part of the food itself.

The extension of current general models of LH function to encompass a role for LH in learning to associate the sensory properties of a food with its rewarding aspects allows us to reinterpret previous data showing that optogenetic stimulation of LH GABA neurons increases an approach to food and food consumption [8, 37]. These studies have shown that stimulation of LH GABA neurons increases time spent in an area of an open field baited with food and food consumption. Considering the present data, it may be that this increase reflects an enhanced representation of a place-food association that affects the learned response to approach the food location and consume food. In support of this interpretation, one study also showed that activity in LH GABA neurons when mice were in the food location increased with experience in the open arena [37]. That is, activity in these neurons appeared to increase as mice learned the location of the food. Whereas this activity was interpreted as reflecting a role for LH GABA in encoding appetitive responses [37], it could equally well reflect the acquisition of associative information linking the sensory stimuli (e.g., cues and places but also smell, taste, texture, etc.) with the rewarding aspects of food consumption, which then allows these stimuli to control appetitive behaviors.

Inhibition of LH GABA Terminals in VTA during Cue Presentation and Not Reward Facilitates Learning of Cue-Reward Associations

The last experiment demonstrated that inactivation of the terminals of LH GABA neurons in VTA during cue presentation facilitated learning. This paradoxical effect can be understood if cue-evoked reward predictions acquired by the LH GABA neurons are sent to VTA to modulate dopaminergic error signaling [36]. According to this hypothesis, inhibition of the projections from LH GABA neurons to the VTA during the reward-paired cue deprived the VTA of the cue-elicited expectation of reward accumulating in LH GABA neurons, leading to the preservation of prediction error signaling by VTA dopamine neurons at the time of reward. Because activity in LH GABA neurons—and other neuronal structures involved in learning, e.g., basolateral amygdala (BLA) [38–41] and nucleus accumbens (NaCC) [19, 42]—remained online during inhibition of their terminals in VTA, they would be free to store the enhanced learning about the cue caused by the excessive prediction errors across conditioning. Thus, information acquired by LH GABA neurons during Pavlovian conditioning acts not only to support real-time food-seeking behavior, at the level of the LH, but is also deployed to VTA to adjust learning and affect future responding to the same food associates. This is as it should be if LH GABA neurons are part of a core circuit for acquiring and using associative information.

Importantly, this result is not at odds with recent reports implicating the LH→ VTA pathway in approach to reward [25, 43]. For example, Nieh et al. [25] have shown that optogenetic manipulation of LH neurons projecting to VTA modulates the willingness of mice to cross a shock grid to obtain reward after learning. Interestingly, in this same study, more selective stimulation of the LH GABA projections to VTA failed to produce any change in ongoing behavior. Together with our data, this suggests that the function of LH GABA neurons projecting to VTA in learning and motivation is best described as a circuit that signals reward predictions to the VTA for the purposes of learning, but not for driving behavior.

Notably, the information provided by LH GABA neurons to the VTA is qualitatively different from that provided by other areas that send input regarding to VTA and the dopamine neurons. For example, orbital frontal cortex (OFC) provides VTA with information about complex aspects of the task that must be inferred to predict the future value of reward [44], and the ventral striatum contributes learning about the duration of task states [45]. Contrary to recent suggestions [46], this shows that VTA neurons do receive qualitatively different types of associative information from multiple sources. Understanding how dopaminergic (and other) neurons in the VTA integrate input from the LH GABA neurons and these other sources, and return it to update these various representations, is an important future goal.

STAR★METHODS

Detailed methods are provided in the online version of this paper and include the following:

- KEY RESOURCES TABLE
- CONTACT FOR REAGENT AND RESOURCE SHARING
- EXPERIMENTAL MODEL AND SUBJECT DETAILS
- METHOD DETAILS
  - Characterization of the GAD-Cre rat
  - Behavioral Experiments
  - Validation of the GAD-Cre rat
  - Surgical and histological procedures used in behavioral studies
  - Behavioral Procedures
- QUANTIFICATION AND STATISTICAL ANALYSES
- DATA AND SOFTWARE AVAILABILITY

SUPPLEMENTAL INFORMATION

Supplemental Information includes four figures and two movies and can be found with this article online at http://dx.doi.org/10.1016/j.cub.2017.06.024.

AUTHOR CONTRIBUTIONS

M.J.S., N.J.M., and G.S. conceived the behavioral experiments. M.J.S., N.J.M., and E.J.C. carried out the behavioral experiments and conducted the histological and immunohistochemical procedures. M.J.S. analyzed the behavioral data. C.T.R., Y.J.Z., P.P.K., J.C.N., C.M.-A., M.M., J.P., J.C.S., L.R.W., and B.K.H. conducted experiments related to validation of the

GAD-Cre rat and conducted the associated analyses. M.J.S., N.J.M., Y.N., Y.S., B.K.H., and G.S. wrote the manuscript.

ACKNOWLEDGMENTS

This work was supported by the Intramural Research Program at the National Institute on Drug Abuse (ZIA DA000587). The authors would like to thank Dr. Karl Deisseroth and the Gene Therapy Center at the University of North Carolina at Chapel Hill for providing viral reagents. The opinions expressed in this article are the authors' own and do not reflect the view of the NIH/DHHS.

Received: March 27, 2017
Revised: May 8, 2017
Accepted: June 9, 2017
Published: July 6, 2017

REFERENCES

1. Changizi, M.A., McGehee, R.M.F., and Hall, W.G. (2002). Evidence that appetitive responses for dehydration and food-deprivation are learned. Physiol. Behav. *75*, 295–304.
2. Hall, W.G. (1979). Feeding and behavioral activation in infant rats. Science *205*, 206–209.
3. Hall, W.G., Arnold, H.M., and Myers, K.P. (2000). The acquisition of an appetite. Psychol. Sci. *11*, 101–105.
4. Friedman, M.I., and Campbell, B.A. (1974). Ontogeny of thirst in the rat: effects of hypertonic saline polyethylene glycol, and vena cava ligation. J. Comp. Physiol. Psychol. *87*, 37–46.
5. Galef, B.G. (1971). Social effects in the weaning of domestic rat pups. J. Comp. Physiol. Psychol. *75*, 358–362.
6. Balleine, B., and Dickinson, A. (1991). Instrumental performance following reinforcer devaluation depends upon incentive learning. Q. J. Exp. Psychol. B *43*, 279–296.
7. Balleine, B.W., and Dickinson, A. (1998). The role of incentive learning in instrumental outcome revaluation by sensory-specific satiety. Anim. Learn. Behav. *26*, 46–59.
8. Jennings, J.H., Rizzi, G., Stamatakis, A.M., Ung, R.L., and Stuber, G.D. (2013). The inhibitory circuit architecture of the lateral hypothalamus orchestrates feeding. Science *341*, 1517–1521.
9. Stuber, G.D., and Wise, R.A. (2016). Lateral hypothalamic circuits for feeding and reward. Nat. Neurosci. *19*, 198–205.
10. Delgado, J.M., and Anand, B.K. (1953). Increase of food intake induced by electrical stimulation of the lateral hypothalamus. Am. J. Physiol. *172*, 162–168.
11. Hoebel, B.G., and Teitelbaum, P. (1962). Hypothalamic control of feeding and self-stimulation. Science *135*, 375–377.
12. Schwartz, M.W., Woods, S.C., Porte, D., Jr., Seeley, R.J., and Baskin, D.G. (2000). Central nervous system control of food intake. Nature *404*, 661–671.
13. Saper, C.B., Chou, T.C., and Elmquist, J.K. (2002). The need to feed: homeostatic and hedonic control of eating. Neuron *36*, 199–211.
14. Horvath, T.L., and Diano, S. (2004). The floating blueprint of hypothalamic feeding circuits. Nat. Rev. Neurosci. *5*, 662–667.
15. Kenny, P.J. (2011). Reward mechanisms in obesity: new insights and future directions. Neuron *69*, 664–679.
16. Anand, B.K., and Brobeck, J.R. (1951). Localization of a "feeding center" in the hypothalamus of the rat. Proc. Soc. Exp. Biol. Med. *77*, 323–324.
17. Wise, R.A. (1974). Lateral hypothalamic electrical stimulation: does it make animals 'hungry'? Brain Res. *67*, 187–209.
18. Petrovich, G.D., and Gallagher, M. (2007). Control of food consumption by learned cues: a forebrain-hypothalamic network. Physiol. Behav. *91*, 397–403.
19. Kelley, A.E., and Berridge, K.C. (2002). The neuroscience of natural rewards: relevance to addictive drugs. J. Neurosci. *22*, 3306–3311.
20. Kalivas, P.W., and Nakamura, M. (1999). Neural systems for behavioral activation and reward. Curr. Opin. Neurobiol. *9*, 223–227.
21. Marchant, N.J., Hamlin, A.S., and McNally, G.P. (2009). Lateral hypothalamus is required for context-induced reinstatement of extinguished reward seeking. J. Neurosci. *29*, 1331–1342.
22. Marchant, N.J., Kaganovsky, K., Shaham, Y., and Bossert, J.M. (2015). Role of corticostriatal circuits in context-induced reinstatement of drug seeking. Brain Res. *1628* (Pt A), 219–232.
23. Sternson, S.M., Nicholas Betley, J., and Cao, Z.F.H. (2013). Neural circuits and motivational processes for hunger. Curr. Opin. Neurobiol. *23*, 353–360.
24. Wise, R.A. (1969). Plasticity of hypothalamic motivational systems. Science *165*, 929–930.
25. Nieh, E.H., Matthews, G.A., Allsop, S.A., Presbrey, K.N., Leppla, C.A., Wichmann, R., Neve, R., Wildes, C.P., and Tye, K.M. (2015). Decoding neural circuits that control compulsive sucrose seeking. Cell *160*, 528–541.
26. Wise, R.A., and Albin, J. (1973). Stimulation-induced eating disrupted by a conditioned taste aversion. Behav. Biol. *9*, 289–297.
27. Harris, G.C., Wimmer, M., and Aston-Jones, G. (2005). A role for lateral hypothalamic orexin neurons in reward seeking. Nature *437*, 556–559.
28. Burton, M.J., Rolls, E.T., and Mora, F. (1976). Effects of hunger on the responses of neurons in the lateral hypothalamus to the sight and taste of food. Exp. Neurol. *51*, 668–677.
29. Ono, T., Nishino, H., Sasaki, K., Fukuda, M., and Muramoto, K.-I. (1981). Monkey lateral hypothalamic neuron response to sight of food, and during bar press and ingestion. Neurosci. Lett. *21*, 99–104.
30. Valenstein, E.S., Cox, V.C., and Kakolewski, J.W. (1968). Modification of motivated behavior elicited by electrical stimulation of the hypothalamus. Science *159*, 1119–1121.
31. Berridge, K.C., and Valenstein, E.S. (1991). What psychological process mediates feeding evoked by electrical stimulation of the lateral hypothalamus? Behav. Neurosci. *105*, 3–14.
32. Petrovich, G.D., Holland, P.C., and Gallagher, M. (2005). Amygdalar and prefrontal pathways to the lateral hypothalamus are activated by a learned cue that stimulates eating. J. Neurosci. *25*, 8295–8302.
33. Ragan, T., Kadiri, L.R., Venkataraju, K.U., Bahlmann, K., Sutin, J., Taranda, J., Arganda-Carreras, I., Kim, Y., Seung, H.S., and Osten, P. (2012). Serial two-photon tomography for automated ex vivo mouse brain imaging. Nat. Methods *9*, 255–258.
34. Mahn, M., Prigge, M., Ron, S., Levy, R., and Yizhar, O. (2016). Biophysical constraints of optogenetic inhibition at presynaptic terminals. Nat. Neurosci. *19*, 554–556.
35. Ghirlanda, S., and Enquist, M. (2003). A century of generalization. Anim. Behav. *66*, 15–36.
36. Schultz, W., Dayan, P., and Montague, P.R. (1997). A neural substrate of prediction and reward. Science *275*, 1593–1599.
37. Jennings, J.H., Ung, R.L., Resendez, S.L., Stamatakis, A.M., Taylor, J.G., Huang, J., Veleta, K., Kantak, P.A., Aita, M., Shilling-Scrivo, K., et al. (2015). Visualizing hypothalamic network dynamics for appetitive and consummatory behaviors. Cell *160*, 516–527.
38. Balleine, B.W., and Killcross, S. (2006). Parallel incentive processing: an integrated view of amygdala function. Trends Neurosci. *29*, 272–279.
39. Blundell, P., Hall, G., and Killcross, S. (2003). Preserved sensitivity to outcome value after lesions of the basolateral amygdala. J. Neurosci. *23*, 7702–7709.
40. Killcross, S., and Coutureau, E. (2003). Coordination of actions and habits in the medial prefrontal cortex of rats. Cereb. Cortex *13*, 400–408.
41. Sharpe, M.J., and Schoenbaum, G. (2016). Back to basics: making predictions in the orbitofrontal-amygdala circuit. Neurobiol. Learn. Mem. *131*, 201–206.

42. Day, J.J., Roitman, M.F., Wightman, R.M., and Carelli, R.M. (2007). Associative learning mediates dynamic shifts in dopamine signaling in the nucleus accumbens. Nat. Neurosci. *10*, 1020–1028.
43. Barbano, M.F., Wang, H.-L., Morales, M., and Wise, R.A. (2016). Feeding and reward are differentially induced by activating GABAergic lateral hypothalamic projections to VTA. J. Neurosci. *36*, 2975–2985.
44. Takahashi, Y.K., Roesch, M.R., Stalnaker, T.A., Haney, R.Z., Calu, D.J., Taylor, A.R., Burke, K.A., and Schoenbaum, G. (2009). The orbitofrontal cortex and ventral tegmental area are necessary for learning from unexpected outcomes. Neuron *62*, 269–280.
45. Takahashi, Y.K., Langdon, A.J., Niv, Y., and Schoenbaum, G. (2016). Temporal specificity of reward prediction errors signaled by putative dopamine neurons in rat VTA depends on ventral striatum. Neuron *91*, 182–193.
46. Tian, J., Huang, R., Cohen, J.Y., Osakada, F., Kobak, D., Machens, C.K., Callaway, E.M., Uchida, N., and Watabe-Uchida, M. (2016). Distributed and mixed information in monosynaptic inputs to dopamine neurons. Neuron *91*, 1374–1389.
47. Gradinaru, V., Zhang, F., Ramakrishnan, C., Mattis, J., Prakash, R., Diester, I., Goshen, I., Thompson, K.R., and Deisseroth, K. (2010). Molecular and cellular approaches for diversifying and extending optogenetics. Cell *141*, 154–165.
48. Warming, S., Costantino, N., Court, D.L., Jenkins, N.A., and Copeland, N.G. (2005). Simple and highly efficient BAC recombineering using galK selection. Nucleic Acids Res. *33*, e36.
49. Shimshek, D.R., Kim, J., Hübner, M.R., Spergel, D.J., Buchholz, F., Casanova, E., Stewart, A.F., Seeburg, P.H., and Sprengel, R. (2002). Codon-improved Cre recombinase (iCre) expression in the mouse. Genesis *32*, 19–26.
50. Filipiak, W.E., and Saunders, T.L. (2006). Advances in transgenic rat production. Transgenic Res. *15*, 673–686.
51. Henderson, M.J., Wires, E.S., Trychta, K.A., Richie, C.T., and Harvey, B.K. (2014). SERCaMP: a carboxy-terminal protein modification that enables monitoring of ER calcium homeostasis. Mol. Biol. Cell *25*, 2828–2839.
52. Paxinos, G.W.C. (1998). The Rat Brain in Stereotaxic Coordinates (Academic Press).
53. Chang, C.Y., Esber, G.R., Marrero-Garcia, Y., Yau, H.J., Bonci, A., and Schoenbaum, G. (2016). Brief optogenetic inhibition of dopamine neurons mimics endogenous negative reward prediction errors. Nat. Neurosci. *19*, 111–116.
54. Sharpe, M.J., and Killcross, S. (2014). The prelimbic cortex contributes to the down-regulation of attention toward redundant cues. Cereb. Cortex *24*, 1066–1074.
55. Sharpe, M.J., and Killcross, S. (2015). The prelimbic cortex directs attention toward predictive cues during fear learning. Learn. Mem. *22*, 289–293.
56. Sharpe, M.J., and Killcross, S. (2015). The prelimbic cortex uses higher-order cues to modulate both the acquisition and expression of conditioned fear. Front. Syst. Neurosci. *8*, 235.
57. Zhang, F., Wang, L.-P., Brauner, M., Liewald, J.F., Kay, K., Watzke, N., Wood, P.G., Bamberg, E., Nagel, G., Gottschalk, A., and Deisseroth, K. (2007). Multimodal fast optical interrogation of neural circuitry. Nature *446*, 633–639.
58. Jones, J.L., Esber, G.R., McDannald, M.A., Gruber, A.J., Hernandez, A., Mirenzi, A., and Schoenbaum, G. (2012). Orbitofrontal cortex supports behavior and learning using inferred but not cached values. Science *338*, 953–956.

STAR★METHODS

KEY RESOURCES TABLE

REAGENT or RESOURCE	SOURCE	IDENTIFIER
Bacterial and Virus Strains		
Adeno-Associated Virus: AAV1 EF1a DIO Mem-AcGFP	This work	NIDA Optogenetics and Transgenic Technology Core
Adeno-Associated Virus: AAV1 EF1a DIO Nuc-eYFP	This work	NIDA Optogenetics and Transgenic Technology Core
Adeno-Associated Virus: AAV- EF1α-DIO-eNpHR3.0-eYFP	[47]	UNC Vector Core
Adeno-Associated Virus: AAV-EF1α-DIO-eYFP	[47]	UNC Vector Core
Experimental Models: Organisms/Strains		
Rat: LE-Tg(GAD1-iCre)3Ottc	This work	RRRC#751; RGD ID 9588593
Oligonucleotides		
iCRE F738 GTTCTGCCGGGTCAGAAAGAATGGT	This work	N/A
bGHpA R30 GGCTGGCAACTAGAAGGCAC	This work	N/A
GAD1 R167672 GGTGCCCTGAGAGTAACCTC	This work	N/A
Recombinant DNA		
Plasmid - AAV EF1a DIO Mem-AcGFP	This work	Addgene #75081
Plasmid - AAV EF1a DIO Nuc-eYFP	This work	Addgene #75082
Bacterial Artificial Chromosome – rat GAD1	BACPAC Resource Center, Children's Hospital Oakland Research Institute	CH230-24D16
Bacterial Artificial Chromosome – rat GAD1-iCre	This work	NIDA Optogenetics and Transgenic Technology Core, pOTTC335

CONTACT FOR REAGENT AND RESOURCE SHARING

Further information and requests for resources and reagents should be directed to and will be fulfilled by Geoffrey Schoenbaum (geoffrey.schoenbaum@nih.gov). Requests for the transgenic rat can be referred to Brandon Harvey (brandon.harvey@nih.gov).

EXPERIMENTAL MODEL AND SUBJECT DETAILS

- As stated multiple times below in various relevant places, all experimental procedures were conducted in accordance with NIH Guidelines and were approved by the Animal Care and Use Committee at the NIDA-IRP.
- The experiments described here utilized both male and female Long-Evans rats, of approximately 2-6 months of age.
- Health/Immune Status: healthy, normal immune status
- Whether subjects were involved in previous procedures: no
- Genotype of experimental animals: the transgenic model was developed on a Long-Evans background
- Species/strain of experimental models: the transgenic model was developed on a Long-Evans background
- Husbandry conditions of experimental animals: breeding was conducted according to standard procedures, approved by the Institutional Animal Care and Use Committee.
- Housing conditions of experimental animals: animals were housed in an accredited vivarium on site at the NIDA-IRP.

METHOD DETAILS

Characterization of the GAD-Cre rat

Transgenic DNA constructs

The GAD1-Cre BAC (pOTTC335) was recombineered using the bacterial artificial chromosome (BAC) clone #CH230 - 24D16 (Children's Hospital Oakland Research Institute, Oakland, CA) which carries a 245 kilobase fragment of rat genomic DNA containing the Gad1 locus flanked by endogenous sequences (167 kilobases upstream and kilobases downstream (Figure 1A). The original BAC

was electroporated into the lambda Red recombination strain SW102 and selected on LB+Chloramphenicol [48]. An isolated colony was heat shocked and electroporated with the GAD1 targeting donor template, a PCR product consisting of a Cre gene cassette encoding iCre [49], the bovine growth hormone poly-adenylation signal, and a galK selectable marker, flanked by homologous arms corresponding to the 50 nucleotides flanking each side of the GAD1 start codon. Transformants were selected on MacConkey's plates containing galactose, and screened for targeted integration into GAD1 locus by PCR genotyping and sequencing.

pAAV EF1a DIO Mem-AcGFP (Addgene #75081) was constructed by ligation-independent cloning, using pOTTC591 (Addgene #59134) as a template for PCR amplification and pOTTC374 (Addgene #47626) as a backbone. pAAV EF1a DIO Nuc-eYFP (Addgene #75082) was constructed by ligation-independent cloning, using pOTTC589 (Addgene #59133) as a template for PCR amplification and pOTTC374 (Addgene #47626) as a backbone.

Transgenic rat production

All animal procedures were performed in accordance with National Institutes of Health Animal Care Guidelines. Female Long Evans rats were obtained from Charles River Laboratories. After synchronization of their ovulation cycle, these rats were superovulated and mated as previously described [50]. Embryos were harvested and injected with a 3ng/μL solution of the GAD1-Cre BAC. Injected embryos were incubated until the "blastula stage" and then transfer into a pseudo-pregnant surrogate female. Embryos were carried to term and ear biopsies were genotyped after weening. Three founder lines were identified and tested for copy number by droplet digital PCR (Bio-Rad, Hercules, CA) and co-expression of Cre/GAD1 by RNAScope. Line 3 was designated "LE-Tg(GAD1-iCre)3Ottc" and registered with the Rat Genome Database (#9588591) and deposited at the Rat Resource and Research Center (RRRC#751; University of Missouri, Columbia MO). Herein, "LE-Tg(GAD1-iCre)3Ottc" rats are referred to as "GAD-Cre" rats. Rats were bred as Cre+ carriers by wild-type Long-Evans from Charles River Laboratories.

Genotyping

Two genotyping protocols were used. To identify carriers of iCre with a bGH polyA tail sequence, a 367 bp PCR product resulted from using the forward primer (iCRE F738) 5′GTTCTGCCGGGTCAGAAAGAATGG T3′ and reverse primer (bGHpolyA R30) 5′GGCTGGCAACTAGAAGGCAC3′ after 40 PCR cycles of 94°C −30 s and 68°C – 1 min. To confirm carriers specific to GAD and iCre, the reverse primer (500 nM) was replaced with (GAD1 R167672) 5′GGTGCCCTGAGAGTAACCTC3′ to produce a 2158 bp PCR product after 35 cycles of 94°C −30 s, 65°C – 30 s and 68°C −1 min. All primers used at 500 nM final.

Adeno-associated viral (AAV) vectors

AAV EF1a DIO Mem-AcGFP and AAV EF1a DIO Nuc-eYFP were produced by the NIDA Optogenetics and Transgenic Technology Core (Baltimore, MD) as described previously [51]. AAV- EF1α-DIO-eNpHR3.0-eYFP and AAV-EF1α-DIO-eYFP [47] were obtained from the UNC Vector Core (University of North Carolina at Chapel Hill). Titers for viruses: EF1a DIO Mem-AcGFP (3.9×10^{12} vg/ml), AAV EF1a DIO Nuc-eYFP (1.9×10^{12} vg/ml), AAV- EF1α-DIO-eNpHR3.0-eYFP (3×10^{12}vg/ml) and AAV-EF1α-DIO-eYFP (3×10^{12}vg/ml).

Characterizing GAD-Cre rat by viral injections

Male (n = 3) and one female (n = 1) GAD-Cre rat of approximately 5-6 months of age (300-600 g) were stereotactically injected with cre-dependent AAV vectors, AAV EF1a DIO Mem-AcGFP and AAV EF1a DIO Nuc-eYFP into the lateral hypothalamus (AP:-2.4, ML: ± 3.5@10°; angle, DV:-9.0) and midbrain (AP:-5.8, ML: ± 2.0, DV:-7.4). All coordinates in mm relative to bregma and 1.0 μL was infused via 33 G blunt Nanofil syringe (World Precision Instruments) at a rate of 0.5 mL/min with a 2 min wait before withdrawing the needle. Two-three weeks following injections, rats were euthanized and the brains were removed and frozen in isopentane on dry ice for RNAscope analysis or transcardially perfused with 0.9% saline followed by 4% paraformaldehyde processed for histological fluorescence using microscopy or TissueCyte whole brain imaging. Confocal microscopy of fluorescent protein expression was carried out using Nikon Eclipse E800 upright with a Nikon C2 confocal head and Nikon Elements Software. Low-magnification images of fluorescence were acquired using Olympus MVX10 macro zoom.

Whole-brain imaging using TissueCyte

GAD-Cre rats injected with 0.5 μl AAV1-EF1a-DIO-Mem-AcGFP into right lateral hypothalamus. Two weeks later, rats were transcardially perfused with 4% PFA, brains removed and post-fixed 2 hr and washed with 1xPBS three times. The brain was embedded in 4.5% oxidized agarose (4.5 g agarose in 1xPB solution including 10 mM NacLO4) and incubated in borohydride-borate solution (19 g borax and 3g boric acid to 1 l water, p 9-9.5) for 2-3 hr at room temperature. The brain tissue was positioned on x-y-z stage under a high-speed multiphoton microscope (16x) with integrated vibratome sectioning (TissueCyte 1000, Tissue Vision) and laser (Chameleon Ultra, Coherent Inc). Serial images of 170 coronal sections with interval of 100 μm were automatically taken by TissueCyte software and images were stitched with Fiji software. Using Fiji software, the stitched images were cropped and pixel size (width and height) was scaled up to 50 microns. A proxy for the entire brain volume (blue channel) was extracted from the GFP stack by finding the edges around a binary mask that was thresholded to the level of GFP background fluorescence. The brain volume stack was merged with the GFP stack to create an RGB image which was used to create the 3D projection (360 frames with 1 degree increments).

Behavioral Experiments

Subjects

Fifty-two experimentally naive male (n = 24) and female (n = 28) Long-Evans transgenic rats carrying a GAD-dependent Cre expressing system (NIDA animal breeding facility, see above) were used in the Pavlovian conditioning studies. Rats received bilateral infusions of either NpHR (n = 25) or eYFP (n = 27) into the LH with fibers aimed either at the LH (Experiment 1 and 2) or the VTA (Experiment 3). Rats were maintained on a 12 hr light-dark cycle, where all behavioral experiments took place during the light cycle. Rats

had ad libitum access to food and water unless undergoing the behavioral experiment during which they received ~85% of their free-feeding body weight. All experimental procedures were conducted in accordance with Institutional Animal Care and Use Committee of the US National Institute of Health guidelines. Rats were randomly allocated to experimental conditions according to an equal distribution of age, sex, and weight.

Validation of the GAD-Cre rat

Identification of orexin neurons

Rinsed Brain slices were first incubated in PBS solution containing 0.3% Triton X-100, 2% NHS for 72 hr, and the primary antibody anti-orexin-A raised in rabbit (1:2000; Phoenix Pharmaceuticals, Inc., Cat #H003-30). After rinses in PBS, tissue was incubated for one hour in a PBS solution containing 0.3% Triton X-100, 2% NHS, and the secondary antibody AF 594 anti-rabbit 1:200 (711-585-152, Jackson ImmunoResearch) at room temperature. Following another round of PBS washes, slices were mounted and cover-slipped with Vectashield H-1400.

Identification of MCH neurons

All procedures were the same as those described above with the exception that the primary antibody used was anti-MCH antibody raised in goat (1:1000; SC-14507; Santa Cruz Biotechnology Inc, Santa Cruz, CA, USA), and the secondary antibody used was AF 594 anti-goat 1:200 (Cat # 705-585-003, Jackson ImmunoResearch).

Quantification of neurons

Tissue from a subset of rats (n = 6) was imaged using iVision (Biovision) software under a 10x microscopic objective using an EXi Aqua camera (QImaging) attached to a Zeiss Axio Imager M2. Each quantified image was derived from 8 images captured at different focal planes and digitally merged using iVision. Bilateral counts of eYFP, MCH and Orexin were analyzed in the LH across three levels of the anterior-posterior plane (AP: −1.8; −2.5; −2.8) by one observer. Cells were counted if their diameter exceeded 25 pixels. Dual-labeled cells were quantified by merging the two cell images in iVision. All brain coordinates were adapted from the Paxinos and Watson atlas [52].

Ex-vivo electrophysiology

Rats were deeply anesthetized with isoflurane (60-90 s) and then rapidly decaptitated. Coronal slices containing lateral hypothalamus were cut in ice-cold solution containing (in mM) 92 NMDG, 20 HEPES, 25 Glucose, 30 $NaHCO_3$, 1.2 NaH_2PO_4, 2.5 KCl, 5 Na-ascorbate, 3 Na-pyruvate, 2 Thiourea, 10 $MgSO_4$, 0.5 $CaCl_2$, saturated with 95% O_2 5% CO_2 (pH 7.3-7.4, ~305 mOsm/kg)] and incubated for 15 min at 35 degrees celsius in the same solution. Slices were allowed to recover for a minimum of 30 min at room temperature in artificial cerebrospinal fluid (ACSF) containing (in mM) 126 NaCl, 2.5 KCl, 1.2 $MgCl_2$, 2.4 $CaCl_2$, 1.2 NaH_2PO_4, 21.4 $NaHCO_3$, 11.1 Glucose, 3 Na-pyruvate, 1 Na-ascorbate, 0.01 DNQX, and 0.05 Picrotoxin. For NpHR experiments, recordings were made at 32-35°C in the same solution which was bath perfused at 2 mL/min. Intracellular solution contained (in mM) 115 K-gluconate, 20 KCl, 1.5 $MgCl_2$, 10 HEPES, 0.025 EGTA, 2 Mg-ATP, 0.2 Na_2-GTP, 10 Na_2-phosphocreatine (pH 7.2-7.3, ~285 mOsm/kg). For IPSC recordings in VTA the intracellular solution contained (in mM) 128 KCl, 20 NaCl, 10 HEPES, 1 MgCl2, 1 EGTA, 0.3 CaCl2, 2 Mg-ATP, 0.25 Na-GTP, 0.01 DNQX. Virus-infected (eYFP+) cells were identified using scanning disk confocal microscopy (Olympus FV1000), and differential interference contrast optics were used to patch neurons. Whole cell current clamp recordings were performed in visually identified neurons in the lateral hypothalamus. For NpHR experiments, a 593 nM laser (OEM laser systesms; maximum output 150 mW) attached to fiber optic cable was used to deliver light to the slice. For ChR2 experiments, a 473 nM laser (OEM laser systems, maximum output 500 mW) attached to fiber optic cable was used to deliver light to the slice. Light intensity of 8-12 mW was used to stimulate NpHR or ChR2 in slice recordings. For experiments shown in Figure 2B (left), current pulses were injected (3000 ms square pulse, 50 pA-120 pA). Half of the time, a 1000 ms light pulse was given during current injection. For experiments shown in Figure 2B (right), a 10 s light pulse was delivered to the slice. For experiments shown in Figure 2D, a 2 ms light pulse was delivered to midbrain slices containing LH terminals. Recordings were discarded if series resistance or input resistance changed >10% throughout the course of the recording. An Axopatch 200B amplifier (Molecular Devices) and Axograph X software (Axograph Scientific) were used to record and collect the data, which were filtered at 10 kHz and digitized at 4-20 kHz.

In situ hybridization-RNAscope

RNA in situ hybridization for glutamate decarboxylase1 (GAD1) mRNA and iCre were performed according to "User Manual for Fresh Frozen Tissue" from RNAscope Multiplex Fluorescent Reagent Kit (Advanced Cell Diagnostics). Specifically, freshly frozen brains were cryosectioned (12 μm) onto Superfrost Plus glass slides (Fisher Scientific) and stored at −80°C. Brain sections were fixed in 10% neutral buffered formalin for 20 min at 4°C, rinsed twice in distilled water, gradually dehydrated for 5 min each in 50%, 70% and twice 100% ethanol. Slides were incubated in 100% ethanol at −20°C overnight. The slides were dried at room temperature (22°C) for 10 min then incubated with pre-treatment IV solution at room temperature for 20 min. After rinsing twice in 1xPBS, 1X target probes for specific GAD1 mRNA and iCre were applied to the brain sections and incubated at 40°C for 2 hr in the HybEZ oven (Advanced Cell Diagnostics). The RNAscope® probe #316401 target region 950-1872 of rat glutamate decarboxylase 1 (NCBI RefSeq# NM-017007.1), #435801 target region 441-1503 of rat glutamate decarboxylase 2(NCBI RefSeq#NM_012563.1), #424541 target region 288-1666 of rat vesicular GABA transporter (NCBI RefSeq#NM_031782.1), #317018 target region 1109-2024 of rat vesicular glutamate transporter 2 (NCBI RefSeq#NM_053427.1), and a custom probe for iCre was used. Sections were treated with preamplifier and amplifier probes by applying AMP1 at 40°C for 30 min, AMP2 at 40°C for 15 min and AMP3 at 40°C for 30 min. Sections were then incubated with AMP4 ALtA 40°C for 15 m. Finally, the nuclei were stained using DAPI for 30 s to stain nuclei (blue color). Washes were performed twice between steps using supplied 1X wash buffer. Fluorescence was imaged for YFP, GAD-1

mRNA probe, iCre mRNA probe and DAPI using Zeiss Axio Imager M2 or Z2. Each image was captured using a EXi Aqua CCD camera (QImaging), or ORCA-Flash4.0 LT sCMOS camera (Hamamatsu), at 20x magnification from 12 μm sections. For Nuc-eYFP and GAD-1 mRNA, GAD2 mRNA, and VGAT mRNA colocalization, a YFP signal associated with DAPI nuclei with three or more mRNA fluorescent dots associated with YFP/DAPI was counted as colocalized. Three sections per region and 3 rats per region were counted. For Cre/GAD1 mRNA colocalization, three Cre mRNA dots associated with single DAPI stained nuclei were assessed as being co-localized.

Surgical and histological procedures used in behavioral studies

Surgical procedures have been described elsewhere [53–56]. Briefly, rats received bilateral infusions of 1μl AAV- EF1α-DIO-eNpHR3.0-eYFP (NpHR) or AAV-EF1α-DIO-eYFP (eYFP) into the LH according to the co-ordinates (mm) relative to bregma, AP: −2.4; ML: ± 3.5; DV: −8.4 (female) and −9.0 (male) at an angle of 10° pointed toward the midline [21]. During this surgery, optic fibers were implanted bilaterally (200μm diameter, Precision Fiber Products, CA) in either the LH [AP: −2.4; ML: ± 3.5; DV: −7.9 (female) and −8.5 (male) at an angle of 10° pointed toward the midline] or the VTA [AP:-5.3; −2.61; DV −7.05 (female) and 7.55 (male) at an angle of 15° pointed toward the midline]. At the end of each experiment, rats were euthanized with an overdose of carbon dioxide and perfused with phosphate buffered saline (PBS) followed by 4% Paraformaldehyde (Santa Cruz Biotechnology Inc., CA). Fixed brains were cut in 40μm sections to examine fiber tip position under a fluorescence microscope (Olympus Microscopy, Japan).

Behavioral Procedures

Apparatus

Training was conducted in 8 standard behavioral chambers (Coulbourn Instruments; Allentown, PA) individually housed in light- and sound-attenuating chambers. Each chamber was equipped with a pellet dispenser that delivered one 45-mg pellet into a recessed magazine when activated. Access to the magazine was detected by means of infrared detectors mounted across the mouth of the recess. The chambers contained an auditory stimulus generator, which delivered a tone and siren stimulus through a common speaker on the top right-hand side of the chamber wall when activated. A computer equipped with Coulbourn Instruments software (Allentown, PA) controlled the equipment and recorded the responses.

Pavlovian conditioning

All conditioned stimuli were 10 s in duration, separated by a variable ITI with a mean of 6 min (range = 4-8 min). Two stimuli were used in these experiments (tone, siren). The physical identity of all stimuli was counterbalanced across rats. Stimulus presentation in all phases of the experiments was also fully counterbalanced. On the first day of behavioral training, the rats received food port training where they learned to retrieve pellets from the magazine. During this session, rats received 30 45-g sucrose pellets (Test Diet, NJ; 5TUT) across a one-hour time period. After food port training, the rats received two behavioral sessions (AM and PM) each day. The rats received 12 (experiments 1 and 2) or 14 (Experiment 3) conditioning sessions each consisting of 6 presentations of the two stimuli. During these sessions, termination of cue presentation was followed 1 s later by delivery of two sucrose pellets, designated the CS+. The other stimulus was presented alone without food, designated the CS-. Following conditioning, rats in Experiment 1 and 2 received a cue test where both stimuli were presented 6 (experiment 1) or 8 times (experiment 2) without food. In Experiment 3, rats continued conditioning with the CS+ and CS- for eight more sessions in the absence of the laser. In Experiment 1 and 3, light (532 nm, 16-18 mW output, Shanghai Laser & Optics Century Co., Ltd) was delivered into either the LH or VTA during cue presentations during conditioning. Light delivery began 500 ms prior to cue onset and continued until 500 ms after cue presentation. This was to ensure that cells were affected by light for the duration of the cue presentation [57]. In Experiment 2, light was delivered according to the same parameters across the cue test only. Analyses were conducted on responding in the last 5 s of cue presentation [53, 58] and analyses on time spent in the port during food presentation were conducted over the 2 s after pellet delivery.

Locomotion

Three experimentally naive male Long-Evans rats carrying a GAD-dependent Cre-expressing system (NIDA animals breeding facility, see main manuscript) were used for the locomotor assays. Rats received bilateral infusions of NpHR aimed at the LH with fibers implanted aiming at the injection site as described in the experimental methods section of the main manuscript. Rats were housed as described above. All experimental procedures were conducted in accordance with the Institutional Animal Care and Use Committee of the US National Institute of Health guidelines. Rats were placed in the chambers used for the Pavlovian conditioning procedure described in the main manuscript which were equipped with four infrared photobeams that recorded a response when the beam was broken (and rat was, therefore, moving around the chamber). Rats received three 25-min locomotor screenings where the laser was presented continuously for a 10 s period 8 times across a session (inter-trial interval between laser periods averaged around a variable 3min mean). Locomotor activity was compared during the laser period to 10 s immediately preceding the onset of the laser and immediately following the offset of the laser. The data were averaged across trials in a session which gave a total of 9 observations for statistical analyses (i.e., each rat had three locomotor scores averaged from each of their three sessions). Data were analyzed as a repeated-measures ANOVA with the three time periods as a factor to compare locomotor activity.

QUANTIFICATION AND STATISTICAL ANALYSES

All statistics were conducted using SPSS 24 IBM statistics package. Generally analyses were conducted using a mixed-design repeated-measures analysis of variance (ANOVA) with the exception of the data represented in Figure 2 which were analyzed using

t tests. All analyses of simple main effects were planned and orthogonal and therefore did not necessitate controlling for multiple comparisons. Data distribution was assumed to be normal but homoscedasticity was not formally tested. With the exception of histological analysis, data collection and analyses were not performed blind to the conditions of the experiments. Sample sizes were chosen on the basis of similar prior experiments which have elicited significant results with a similar number of rats. No formal power analyses was conducted.

DATA AND SOFTWARE AVAILABILITY

All data and custom analytical tools are available on request from the Lead Contact, Geoffrey Schoenbaum (geoffrey.schoenbaum@nih.gov).

Current Biology, Volume *27*

Supplemental Information

Lateral Hypothalamic GABAergic Neurons Encode Reward Predictions that Are Relayed to the Ventral Tegmental Area to Regulate Learning

Melissa J. Sharpe, Nathan J. Marchant, Leslie R. Whitaker, Christopher T. Richie, Yajun J. Zhang, Erin J. Campbell, Pyry P. Koivula, Julie C. Necarsulmer, Carlos Mejias-Aponte, Marisela Morales, James Pickel, Jeffrey C. Smith, Yael Niv, Yavin Shaham, Brandon K. Harvey, and Geoffrey Schoenbaum

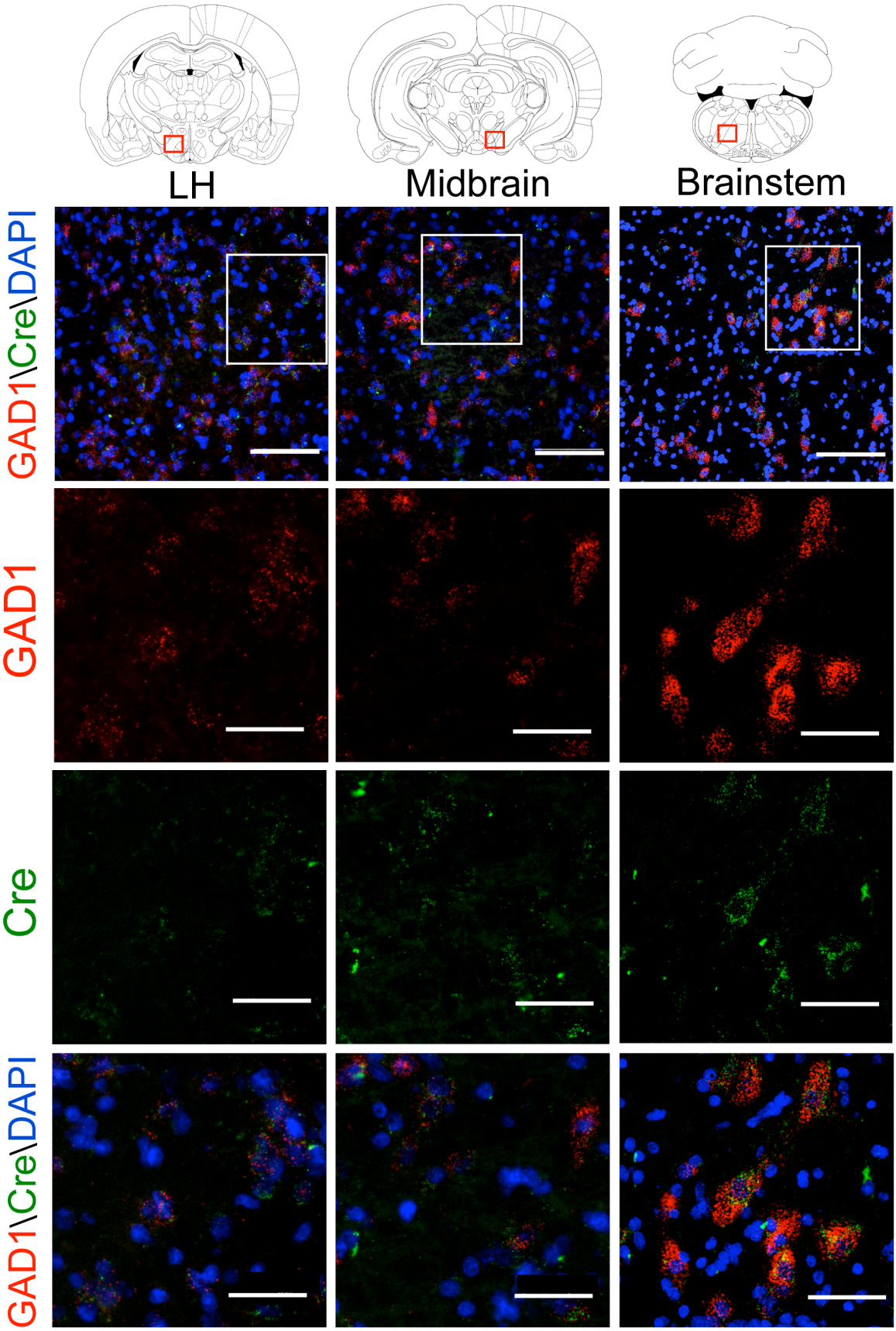
LH
Midbrain
Brainstem
GAD1\Cre\DAPI
GAD1
Cre
GAD1\Cre\DAPI

Figure S1. GAD1 mRNA colocalizes with Cre-recombinase mRNA in the GAD-Cre rat line. Related to Figure 1. Fluorescent RNA in situ hybridization for GAD1 (red) and Cre (green) mRNA shows colocalization of Cre and GAD1 in brain regions expressing GAD1. Top row shows merged images of GAD1 mRNA (red), Cre mRNA (green) and DAPI (nuclei; blue), scale bar 120µm. Inset square is shown at higher magnification below (scale bar=40µm), and separated into separate channels for GAD1 mRNA (red) and Cre mRNA (green). Percentage of GAD1+ cells co-expressing Cre in LH (85±6%), midbrain (76±11%), and medullary reticular formation in the brainstem (87±6%). Counts are means averaged from 3 rats (three sections per region).

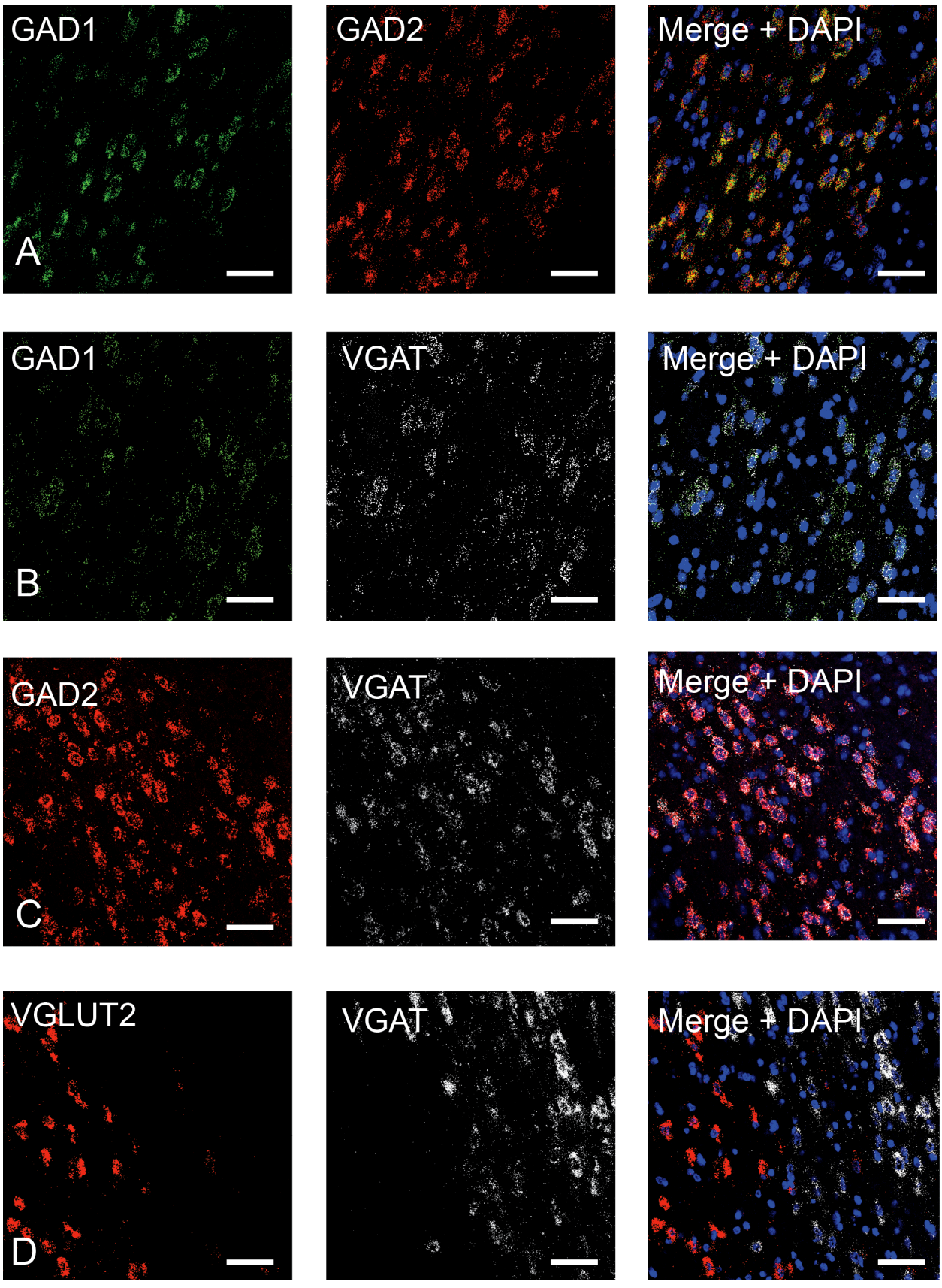
GAD1
A
GAD2
Merge + DAPI
GAD1
B
VGAT
Merge + DAPI
GAD2
C
VGAT
Merge + DAPI
VGLUT2
D
VGAT
Merge + DAPI

Figure S2. Colocalization of GAD1 mRNA with other GABAergic markers (GAD2 and VGAT) and glutamatergic marker (VGLUT2) in LH using RNAscope. Related to Figure 1. (A) GAD1 mRNA (green) and GAD2 mRNA (red) colocalize in 100% of cells **(B)** GAD1 mRNA (green) and VGAT mRNA (white) colocalize in 100% of cells **(C)** GAD2 mRNA (red) and VGAT mRNA (white) colocalize in 99±1% of cells **(D)** VGLUT2 mRNA (red) showed less than 1% colocalization with VGAT mRNA (white) indicating GAD1 cells in LH have a GABAergic phenotype. Total DAPI-stained nuclei (blue) shown in merged images. Scale bar = 50μm.

Midbrain Injection
A
B
posterior striatum
Nuc YFP protein
LH
GAD1 mRNA
VTA
Merge + DAPI
vlPAG

Figure S3. AAV-mediated Cre-dependent expression of nuclear- or membrane-localized YFP following injection into the midbrain. Related to Figure 3. (A) AAV EF1a DIO Nuc-eYFP, Cre-dependent expression of a nuclear localized YFP, was stereotactically injected into the midbrain and tissue was examined 2-3 weeks following injection of Nuc-eYFP fluorescence. Images of coronal brain sections show distribution of Nuc-eYFP fluorescence in the midbrain (top row, scale bar =1mm). Tissue sections expressing Nuc-eYFP were colabeled by fluorescence RNA in situ hybridization for GAD1 (red, third row) and compared with nuclear YFP fluorescence (yellow, second row; scale bar=20µm for rows 2-4), **(B)** Projections from virally-transduced GABAergic neurons originating in the midbrain. Sections are ordered anterior-posterior in the brain from top-bottom in columns. AAV1-EF1a-DIO-mem-AcGFP was injected into the midbrain (1µl) and whole brains were analyzed using the TissyeCyte imaging system two weeks after injection. Scale bar =2mm.

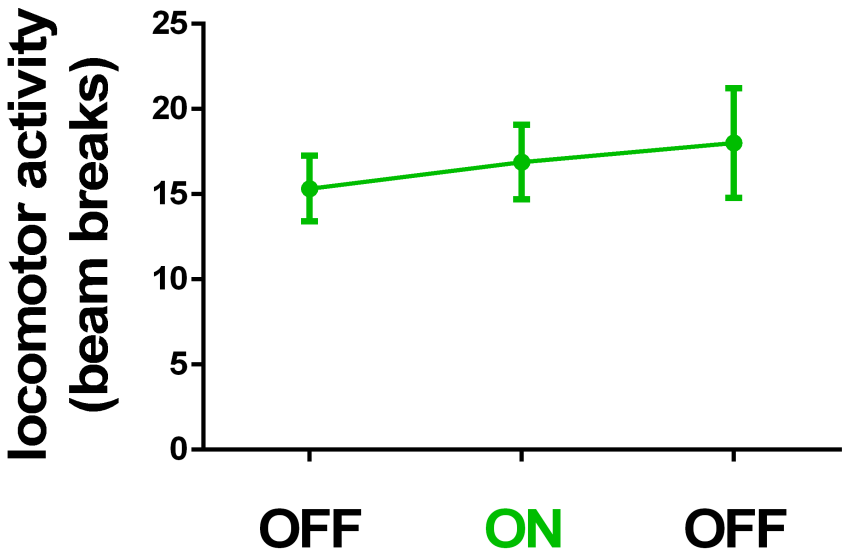

Figure S4. Optogenetic inhibition of LH GABA neurons does not alter spontaneous locomotor activity. Related to Figure 5 and 6. Graphs represent the number of crossings across an infra-red beam (i.e. beam breaks; ±SEM) in the 10-s preceding, during, and after 10-s laser-mediated inhibition of LH GABA neurons. Rats were allowed to move freely around an operant chamber. LH GABA neurons were inhibited using the same parameters as those of experiment 1, 2 and 3. Locomotor activity was unchanged by laser-mediated inhibition of LH GABA neurons (*F*s<1).